POLITECNICO DI TORINO
Repository ISTITUZIONALE

DIDEM - An integrated model for comparative health damage costs calculation of air pollution

(Article begins on next page)

19 April 2024

Accepted Manuscript

DIDEM - An integrated model for comparative health damage costs calculation of air pollution

Marco Ravina, Deborah Panepinto, Maria Chiara Zanetti
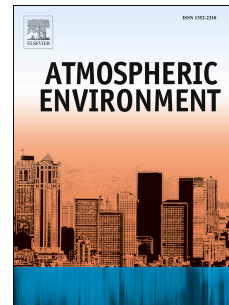
Please cite this article as: Ravina, M., Panepinto, D., Zanetti, M.C., DIDEM - An integrated model for comparative health damage costs calculation of air pollution, *Atmospheric Environment* (2017), doi: 10.1016/j.atmosenv.2017.11.010.

- NO$_x$, PM$_{2.5}$, PM$_{10}$ emission flow (present and alternative scenario)
- Emission source geometry and location (present and alternative scenario)

DIDEM
integrated model

CALPUFF
dispersion model

- Delta-concentration maps of NO$_x$, PM$_{2.5}$, PM$_{10}$
- Delta-external costs distribution map
- Tables of overall delta-external costs, including uncertainty estimates

Emission scenarios

Estimation of delta-concentrations

NOx
conc.
µg/m3

▲ Moncalieri plant
+ Torino Nord plant
◆ BIT plant
● Politecnico plant
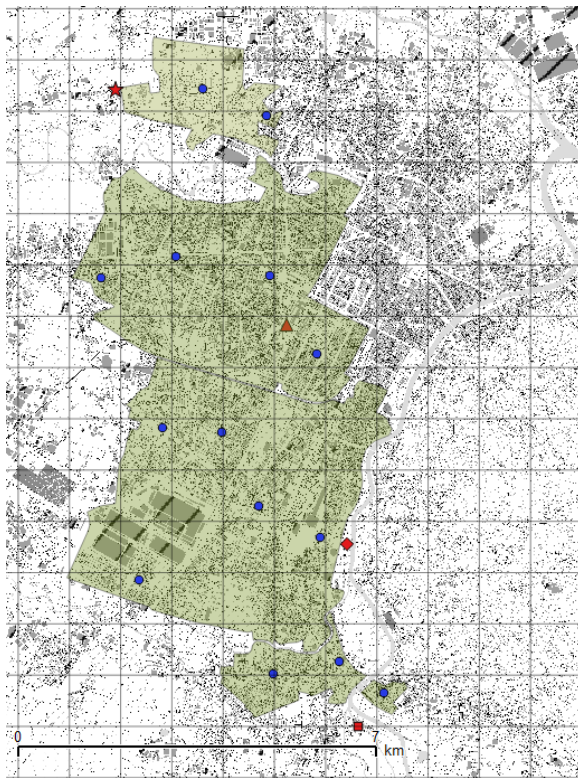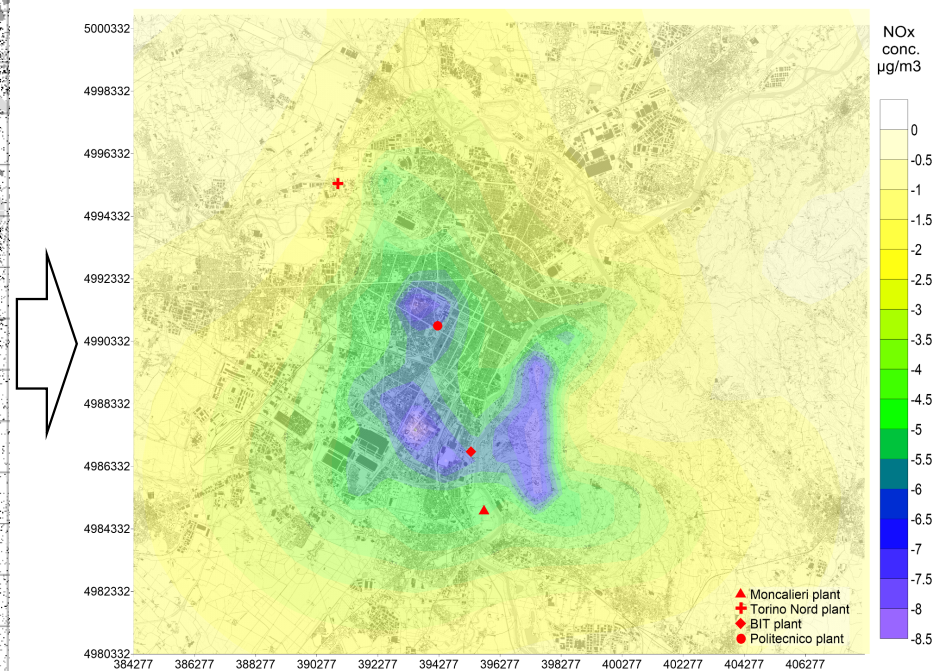
Calculation of delta-external costs

Confidence level on CRF data (Setting)	Delta external costs MEAN (€/y)	
	€/y	€$_{cent}$/kWh
High (Setting 1)	- 8,550,000	-0.472
Medium (Setting 2)	- 58,815,000	-3.244

1   DIDEM - An integrated model for comparative health damage costs calculation of air pollution
2
3   Marco Ravina*, Deborah Panepinto, Maria Chiara Zanetti
4
5   * Corresponding author
6

7   Marco Ravina
8   DIATI (Department of Engineering for Environment, Land and Infrastructures)
9   Politecnico di Torino
10   Corso Duca degli Abruzzi, 24
11   10129 Torino, Italy
12   Phone +39 011 0907632
13   Fax +39 011 0907699
14   marco.ravina@polito.it
15
16   Deborah Panepinto
17   DIATI (Department of Engineering for Environment, Land and Infrastructures)
18   Politecnico di Torino
19   Corso Duca degli Abruzzi, 24
20   10129 Torino, Italy
21   Phone +39 011 0907660
22   Fax +39 011 0907699
23   deborah.panepinto@polito.it
24
25   Maria Chiara Zanetti
26   DIATI (Department of Engineering for Environment, Land and Infrastructures)
27   Politecnico di Torino
28   Corso Duca degli Abruzzi, 24
29   10129 Torino, Italy
30   Phone +39 011 0907696
31   Fax +39 011 0907699
32   mariachiara.zanetti@polito.it
33

34   **Abstract**

35   Air pollution represents a continuous hazard to human health. Administration, companies and
36   population need efficient indicators of the possible effects given by a change in decision, strategy
37   or habit. The monetary quantification of health effects of air pollution through the definition of
38   external costs is increasingly recognized as a useful indicator to support decision and information
39   at all levels. The development of modelling tools for the calculation of external costs can provide
40   support to analysts in the development of consistent and comparable assessments. In this paper,
41   the DIATI Dispersion and Externalities Model (DIDEM) is presented. The DIDEM model calculates
42   the delta-external costs of air pollution comparing two alternative emission scenarios. This tool
43   integrates CALPUFF's advanced dispersion modelling with the latest WHO recommendations on
44   concentration-response functions. The model is based on the impact pathway method. It was
45   designed to work with a fine spatial resolution and a local or national geographic scope. The
46   modular structure allows users to input their own data sets. The DIDEM model was tested on a
47   real case study, represented by a comparative analysis of the district heating system in Turin, Italy.

48 Additional advantages and drawbacks of the tool are discussed in the paper. A comparison with
49 other existing models worldwide is reported.
50
51

52 **Keywords:** air pollution, impact pathway, modelling, health, external costs, heating network
53

54 **Abbreviations**
55 ARPA Piedmont's Regional Agency for Environmental Protection
56 BenMAP Environmental Benefits Mapping and Analysis Program
57 CALPUFF California Puff Model
58 CHP Combined heat and power
59 CRF Concentration – response function
60 DeNOx Selective catalytic reduction for nitrogen oxides removal
61 DEHM Danish Eulerian Hemispheric Model
62 DH District heating
63 DIATI Department of Engineering for Environment, Land and Infrastructures, Turin Polytechnic,
64 Italy
65 DIDEM DIATI Dispersion and Externalities Model
66 EMEP European Monitoring and Evaluation Programme
67 EEA European Environmental Agency
68 EVA Economic Valuation of Air pollution
69 EU European Union
70 GIS Geographic information system
71 GUI Graphical User's Interface
72 HIA Health Impact Assessment
73 HMDB Health Mortality and Morbidity Database
74 HFA-DB Health for All Database
75 HRAPIE Health risks of air pollution in Europe
76 IPA Impact pathway approach
77 kWh_t kWh of thermal energy
78 kWh_{el} kWh of electrical energy
79 LEAP-IBC Long-range Energy Alternatives Planning System - Integrated Benefits Calculator
80 LCA Life Cycle Assessment
81 LPG Liquefied petroleum gases
82 MWh_t MWh of thermal energy
83 MWh_{el} MWh of electrical energy
84 NEEDS New Energy Externalities Developments for Sustainability
85 NewExt New Elements for the Assessment of External Costs from Energy Technologies
86 NO_x nitrous oxides
87 O_3 ozone
88 OML Operational Meteorological Air quality model
89 $PM_{2.5}$ particulate matter <2.5 μm
90 PM_{10} particulate matter <10 μm
91 REVIHAAP Review of evidence on health aspects of air pollution
92 TM5-FASST Tracer model 5, Fast Scenario Screening Tool
93 TSP Total suspended particulate
94 US EPA United States Environmental Protection Agency
95 UTM ED50 Universal Transverse of Mercator, European Datum 1950

96 WHO World Health Organization
97
98   1. INTRODUCTION
99 Although several natural sources (volcanoes, fire, etc.) may release pollutants in the environment,
100 anthropogenic activities are the major cause of environmental air pollution. Hazardous chemicals
101 can escape to the environment by accident, or during the usual operation of industrial facilities
102 and other activities. In both cases, adverse effects on human health and the environment may be
103 observed. By definition, an air pollutant is any substance which may harm humans, animals,
104 vegetation or material. As far as humans are concerned, air pollutants represent a potential
105 hazard to human health. The determination of human health risk connected to air pollution
106 impacts is based on clinical, epidemiological, and/or animal studies, which define how an exposure
107 to a substance is associated with health effects (Kampa and Castanas, 2008).
108 Impacts of air pollution may be observed both at the local and the global scale. At the global scale,
109 greenhouse gas emission generates impacts on the climate system, bringing changes in
110 temperature and weather patterns (Kirtman et al., 2013), crop loss, and increased incidence of
111 certain diseases. At the local scale, the emission of macro- and micro-pollutants generates impacts
112 on humans and ecosystems (Panepinto et al., 2014). These unexpected or unwanted impacts are
113 defined as externalities, i.e. those effects on the wellbeing of an unrelated group or individual
114 outside the market mechanism that controls the price of energy. External costs, or damage costs,
115 are the monetary value of externalities.
116 To quantify and compare environmental impacts, LCA (Life Cycle Assessment) methods are the
117 most widely used tools at present. LCA analysis consider all the process steps, including resource
118 consumption, conversion systems, and residual and waste re-immission into the environment
119 (Blengini et al., 2011). Beside LCA methods, other important tools, such as models for the
120 calculation of environmental balances, or pollutant dispersion models, are used. Many studies
121 about these latter are reported in bibliography, including local case studies (Viggiano et al., 2014a),
122 or methodological dissertations (Viggiano et al., 2014b).
123 Considering health effects of air pollution, decades of toxicological, clinical and epidemiological
124 research support the association between exposure to ambient air pollution and detrimental
125 human health effects, including respiratory disease, cardiovascular disease, and premature death
126 (Anenberg et al., 2016). Driven by these research findings, many countries issued strict regulation
127 on ambient concentration limits of air pollutants, in particular for particulate matter, ozone,
128 nitrogen oxide sulphur oxide and carbon monoxide. The definition of the regulation limits is based
129 on technical and scientific evidence, including estimates of the total pollution health burden posed
130 by the pollutants at current concentrations, as well as the health benefits of reducing air pollution
131 levels.
132 Health impact and health burden assessment depend strongly on air pollution epidemiology and
133 exposure science. Recent advances in these two disciplines have improved the cross-linkage of
134 atmospheric science and epidemiology, allowing analysts to quantify an increasing number of
135 health outcomes in far greater detail than was previously possible.
136 A variety of studies have quantified health impacts associated with air pollution at global (Lim et
137 al., 2010; Cohen et al., 2004; Anenberg et al., 2010; Chambliss et al., 2014), regional (Aneneberg et
138 al., 2009; Likhvar et al., 2015) national (Hubbell et al., 2005; He et al., 2010; Nawadha, 2013) and
139 local scale (Wesson et al., 2010; Fann et al., 2011; Guttikunda and Jawahar, 2012; Kheirbeck et al.,
140 2013). Comparative analysis of health effects under different emission reduction scenarios has
141 been the basis supporting air quality policy development in the European Union (Holland et al.,
142 2005; Amann, 2013), United States (US EPA, 2012) and other countries.

143 Several modelling tools have been developed for calculating health effects and external costs of
144 air pollution. The use of modelling tools has the advantage of supporting analysts in the
145 development of assessment, and offers consistency and comparability among the analysis. These
146 tools have been often designed for a particular objective, and vary in methodological approach,
147 technical complexity, geographical scope, resolution and other factors, such as usability and
148 accessibility (Anenberg et al., 2016). One of the most recognized and used method of analysis is
149 the impact pathway approach, first developed within the ExternE project series (University of
150 Stuttgart; European Commission, 2005; Figure 1). Impact pathway assessment is a bottom-up-
151 approach in which environmental benefits and costs are estimated by following the pathway from
152 source emissions via quality changes of air, soil and water to physical impacts, before being
153 expressed in monetary benefits and costs (European Commission, 1995; Rabl and Spadaro, 1999;
154 Holland, 2014a).

155 At present, the main challenge in modelling health effects and costs of air pollution is the
156 quantification of the overall uncertainty associated to the assessment chain. Such uncertainty may
157 be limited by improving one of the key steps of the methodology (air quality modelling, exposure
158 modelling, impact assessment or monetary valuation).

159 In this paper, a new integrated tool for the calculation of environmental impacts, human health
160 effects and external costs associated to air pollution is presented. This model has been conceived
161 to quantify and minimize the overall uncertainty, by incorporating the following features:

- The integration of a detailed and advanced pollutant dispersion model (CALPUFF) with the
163 calculation of health concentration-response functions (CRFs), implemented following the
164 latest WHO recommendations;
- The implementation of different confidence levels on CRFs data reported by the WHO,
166 resulting in a precise estimation of uncertainty associated to the calculation of health
167 effects;
- The implementation of updated monetary values of health effects introduced by the EU's
169 Clean Air Policy Package.

170 This model was developed at the Department of Engineering for Environment, Land and
171 Infrastructures (DIATI) of Turin Polytechnic, Italy. It is referred as the DIDEM model (DIATI
172 Dispersion and Externalities Model). The DIDEM model was designed to perform an analysis of
173 external health impacts and costs by comparing two or more operating scenarios. DIDEM model
174 was conceived to work with fine spatial resolution and a local geographic scope (cities, metropolis
175 or similar areas). DIDEM model can be used to compare the compatibility of different industrial
176 options, but also various aspects, such as local policy planning or forecasting scenarios.

177 The main structure and operation of DIDEM model is reported in the following sections. The
178 DIDEM model was tested on a real case study, i.e. the environmental analysis of the district
179 heating system of Turin, a town located in the north-west of Italy.

180
181   2. Methodology
182

183 The DIATI integrated dispersion and externalities model (DIDEM) calculates the environmental
184 impacts and the external costs associated to the comparative analysis of emission scenarios. In
185 this paper, the term external costs refers to the marginal health damage costs, i.e. those costs
186 generated by the effects on human health resulting from an extra unit of pollutant concentration.
187 Comparative analysis is performed comparing the present situation to an alternative operating
188 energy scenario.

189 The DIDEM model is based on the impact pathway approach (IPA, Figure 1). The model links the
190 simulation of pollutants dispersion with CALPUFF model to the concentration-exposure-response

191 functions provided by latest WHO recommendations (WHO, 2013a; WHO, 2013b). Monetary
192 values are associated to the incremental incidence of disease calculated. This tool was designed to
193 cover a regional scope, i.e. the EU community. Since it allows a spatial resolution down to 1 km or
194 less, it can be employed at the local scale, e.g. for IPA analysis on large cities.
195 The DIDEM model was developed with MATLAB® (Mathworks) and tested on a real case study.
196 The study case is represented by an evaluation of the environmental performance of the district
197 heating network of Turin, the fourth most-populated city in Italy.
198 The methodological concepts at the basis of the model, the model structure and the study case
199 are described in the following.
200
201

202 2.1 Methodological approach
203 The following general equation conceptualizes the calculation of external costs through the impact
204 pathway approach (modified from van der Kamp and Bachmann, 2015):
205

$$C_{i,r} = \sum_r \sum_i [\Delta c_r \times p_r] \times t \times s_{CRi} \times m_i$$

206
207 Equation 1
208
209

210

211 where $C_{i,r}$ represents the damage costs related to health impact i and to domain cell r, given in
212 €$_{base\ year}$; Δc_r is the concentration change of a given pollutant, referred to domain cell r, given in
213 [µg/m^3] and p_r is the number of exposed individuals [person]; t is a factor to account for different
214 assumptions on particle toxicity; s_{CRi} is the slope of the impact function of health impact i, given in
215 [(additional cases)/((µg/m^3) × person × year)], merging information on the risk increase and
216 baseline rate of a given health impact i; and m is the monetary value per case of health impact i,
217 given in [€$_{base\ year}$/case].
218 The terms Δc_r and s_{CRi} in Equation 1 are the driving variables of the calculation. The delta-
219 concentration is the result of the dispersion modelling and represents the level of exposure of the
220 population to a pollutant (cf. Chapter 2.1.1). The impact function, whose slope is s_{CR}, is defined by
221 a concentration-response function (CRF), usually assumed to be linear with respect to
222 concentration changes (cf. Chapter 2.1.2).
223

224 2.1.1 Estimation of delta-concentration
225 The estimation of pollutants impact on the considered area represents the first step in the impact
226 pathway analysis (Figure 1). The simulation of pollutant dispersion, done with the use of numerical
227 models, provides an estimation of the concentration. Delta-concentration is defined by the
228 algebraic sum of concentrations corresponding to present and alternative scenarios. The
229 dispersion model considered in this study is CALPUFF. CALPUFF is a multi-layer, multi-species, non-
230 steady-state puff dispersion model that simulates the effects of time- and space-varying
231 meteorological conditions on pollution transport, transformation, and removal (US EPA, 2011).
232 The modelling system consists of three main components and a set of pre-processing and post-
233 processing programs. The main components of the modelling system are CALMET (a diagnostic
234 three-dimensional meteorological model), CALPUFF (an air quality dispersion model), and
235 CALPOST (a post- processing package). The model includes algorithms for complex orography,
236 subgrid scale effects (such as terrain impingement), as well as longer range effects, such as
237 pollutant removal due to wet scavenging and dry deposition, chemical transformation, and
238 visibility effects of particulate matter concentrations.

239 CALPUFF is a model that simulates puffs of material emitted from modelled sources, reproducing
240 dispersion and transformation processes along the way. Temporal and spatial variations in the
241 selected meteorological fields are explicitly incorporated in the resulting distribution of puffs
242 throughout a simulation period. The primary output files from CALPUFF contain either
243 concentrations or deposition fluxes evaluated at selected receptor locations. CALPOST is used to
244 process these files. For more technical details on the CALPUFF model structure, refer the user's
245 guide (US EPA, 2011).

246 The choice of CALPUFF rather than other dispersion models was given by the need of a costless,
247 well-known and structured instrument, able to run simulations on the largest possible set of
248 modelling scenarios, including complex topographies, variable scale and variable meteorology
249 (Ravina, 2016).

250

251 2.1.2 Definition of concentration-response function
252 In the framework of the European Union's declaration for 2013 as the Year of Air, the WHO
253 Regional Office for Europe coordinated two international projects ("Review of evidence on health
254 aspects of air pollution - REVIHAAP"; WHO 2013b and "Health risks of air pollution in Europe" -
255 HRAPIE; WHO, 2013a) to provide the stakeholders with evidence-based advice on the health
256 aspects of air pollution. New emerging risks to health from air pollution was also documented by
257 these projects. The HRAPIE project report presents the latest available recommendations for the
258 external cost analysis.

259 Here, the pollutant-outcome pairs recommended for cost analysis are classified into two
260 categories:

261 • Group A: pollutant-outcome pairs for which enough data are available to enable reliable
262   quantification of effects;
263 • Group B: pollutant-outcome pairs for which there is more uncertainty about the precision
264   of the data used for quantification of effects.

265 The pollutants considered are $PM_{2.5}$, O_3 and NO_2. Equal toxicity is assigned to each pollutant, so
266 that the term t of Equation 1 is not accounted. Recommendations for CRFs are given in relative
267 risk (RR). The definition of RR for each pollutant-outcome pair is reported in Table 1. The slope of
268 the CRF (s_{CRi} term in Equation 1) for each pollutant-outcome pair i is calculated as:

269

270 $$s_{CRi} = \frac{n_i(RR_i-1)}{p_{tot,i}} \qquad \text{Equation 2}$$

271

272 where n is the average number of occurrences of the health outcome i (cases/year), whose
273 background rates can be found in WHO's mortality and morbidity database, available on-line
274 (WHO HMDB); $p_{tot,i}$ is the background population exposed to health outcome i, also provided on-
275 line by the WHO database (WHO HFA-DB).

276 The HRAPIE project also reports indications on the additivity of effects of pollutant-outcome pairs.
277 To this end, a limited subset of Group A and Group B (named Group A* and Group B* respectively)
278 is defined, to identify those pairs that contribute to the total effect. The calculation of the range of
279 overall costs is thus recommended to be based on the following principles, here referred as setting
280 1 and 2 (WHO, 2013a):

281 • Setting 1 considers a limited set of impacts based on the sum (∑) of Group A*. An
282   uncertainty range is then provided around this estimate. The limits of this uncertainty
283   range are calculated by summing the minimum (or maximum) values of (Group A*; Group
284   A) pollutant-outcome pairs of the same type (e.g. minimum between the long-term

285   exposure to $PM_{2.5}$ of Group A* and the same pair for Group A + minimum between the
286   long-term exposure to NO_x of Group A* and the same pair for Group A + …).

287   • Setting 2 considers a limited set of impacts based on $\sum$ Group A* + $\sum$ Group B*. An
288   uncertainty range is then provided around this estimate. The limits of this uncertainty
289   range are calculated by summing the minimum (or maximum) values of (Group A*; Group
290   A) pollutant-outcome pairs of the same type, added to the minimum (or maximum) values
291   of (Group B*; Group B) pollutant-outcome pairs of the same type.

292 The calculation of external costs as defined by Setting 1 and Setting 2 was implemented in the
293 DIDEM model.

294 For more details on the HRAPIE project findings and recommendations, refer to the complete
295 report (WHO, 2013a)

296

297 2.2 DIDEM model structure

298 The DIDEM model performs the comparative analysis of environmental impacts and external costs
299 of energy scenarios, integrating the simulation of pollutant dispersion with CALPUFF to the HRAPIE
300 project recommendations for the calculation of health damage costs. The user is allowed to input
301 customized emission flows, including both point and area sources, as well as customized data of
302 population exposure.

303 For each scenario, the input to the model is the hourly emission flow of NO_x (as equivalent NO_2),
304 $PM_{2.5}$ and PM_{10}. Ozone formation and evolution is not modelled. The DIDEM model organizes the
305 hourly series in a compatible format to CALPUFF, and executes CALPUFF. Once the CALPUFF
306 simulation is terminated, the DIDEM model extracts and re-formats the output concentration grids
307 and calculates the concentration differences. These latter are passed to the final module
308 calculating the delta-external costs, which represents the core of the model. The DIDEM model
309 provides different outputs (Figure 2):

310   • Grids of concentration difference of NO_x, $PM_{2.5}$ and PM_{10} over the modelling domain. Grids
311   are provided in ASCII format, in order to be manageable with SURFER® software (Golden
312   Softwares) or GIS tools (e.g. QGIS)

313   • Table of five maximum and minimum concentration difference, with the related position in
314   the spatial domain and the time of occurrence;

315   • Grids of distribution of delta external costs over the modelling domain;

316   • Tables reporting the total variation in external costs associated to the considered scenarios.
317   The results reported herein are differentiated depending on the level of confidence of the
318   input health effect/response pairs considered (group A or group A + Group B, see chapter
319   2.1.2). An estimation of uncertainty is also reported.

320 The DIDEM model is composed by the following five integrated modules:

321   • Module 1 (extract.m): emission source data extraction and analysis;

322   • Module 2 (pte_bae_gen.m): CALPUFF set-up and execution;

323   • Module 3 (calpost.m): extraction of CALPUFF output; calculation of average, maximum and
324   minimum concentration difference; generation of delta-concentration grids.

325   • Module 4 (extern.m): calculation of delta-external costs and related uncertainty range.

326 The model can be executed entirely by running a control script (didem.m); in alternative, each
327 module can be run separately (Figure 3). Input and output from each module is reported in Figure
328 2. The modules are described in the following.

329

330 2.2.1 Module 1 – Data extraction, analysis and correction (extract.m)

331 The function/script extract.m collects the data of the emission sources. An analysis and correction
332 of pollutants emission flow is then performed by this module. The script is divided in two sections,

333   one for the present and one for the alternative scenario. For each scenario, the user is first asked
334   to introduce the number of emission sources (ns), the typology (point or area source), the time of
335   start and end of the simulation, the coordinates of the modelling domain (lower-left and upper-
336   right corners) and the number of domain cells (ncell). The following information and data is then
337   required for each source (variables name and unit is reported in brackets):

- Source ID (id);
- Location in UTM ED50 coordinate system (xcoord, ycoord; km). Area sources are defined by 4 couples of coordinates;
- Height and diameter (hei, diam; m). For area sources, the effective radius (effrad; m) is asked instead of the diameter;
- Elevation (elev; meters above sea level);
- Hourly energy production (eprod; MWh);
- Hourly emission temperature (temp; K);
- Hourly exhaust gas speed (vel; m/s). For area sources, the effective rise velocity (effvel; m/s) is asked instead of the exhaust gas speed;
- Hourly NO_x, $PM_{2.5}$ and PM_{10} flow (nox, pm2, pm10; g/s);
- The format of missing value of input data (e.g. -1 or -9999);

350   The script performs an analysis on the hourly emission flows, indicating the ratio of missing values,
351   the maximum values and the standard deviation of non-zero values. The data are plotted on
352   screen to identify possible values outside the trend. The user is then asked to confirm these data
353   or correct them. If a correction option is selected, the missing or out-of-range values are replaced.
354   Substitution is made by multiplying the thermal energy production by the total emission factor of
355   that source. If a valid datum of thermal energy is missing, emission flow is calculated by linear
356   interpolation between previous and next hourly values. Finally, if no valid data is available for
357   interpolation, the script assigns an emission flow equal to zero.
358   The output of Module 1 for each scenario is a set of coordinates (2 x ns for point sources and 8 x
359   ns for area sources), 4 x ns variables, and a matrix of 8760 (hours) x ns (sources) x 6 (variables)
360   values. These variables are transferred to Module 2.

361

362   2.2.2 Module 2 - CALPUFF set up and execution (pte_bae_gen.m)
363   Module 2 is divided in two sections, one for the present and one for the alternative scenario. This
364   script/function reads the complete information on emission sources and generates the input
365   source files to input in CALPUFF. If point source type is selected, the file PTEMARB.DAT is
366   generated. Otherwise, if an area source type is selected the file BAEMARB.DAT is generated. These
367   files are composed by a header, time-invariant records and series of time-varying records (one per
368   hour). For more information about the structure of these input files, refer to CALPUFF user's
369   manual (US EPA, 2011).
370   The input source files are then transferred to CALPUFF model and CALPUFF is executed. The
371   meteorological input files to CALPUFF must be provided by the user. Once the run is terminated,
372   the script transfers CALPUFF output file (CALPUFF.CON) to CALPOST post-processor and executes
373   it. CALPOST model is set to generate 1-hour and 24-hour average concentration grids for each
374   pollutant. In this way, 6 output files are generated for each scenario. Each file contains one grid of
375   ncell size per averaging period. These output files are transferred to Module 3.

376

377   2.2.4 Module 3 – Calculation of average delta-concentrations (calpost.m)
378   Module 3 has the double function of generating delta-concentration grids and the datasets for the
379   calculation of delta-external costs. The input to this script is the time series generated by CALPOST
380   model. The user is first asked to specify the period over the delta-concentrations are calculated,

381 which must be shorter or equal to the period of simulation. The module then overlaps the
382 concentration grids of present and alternative scenario, calculating the difference.

383 The average concentration difference over the specified period is then calculated. As it is
384 requested by the procedure reported in HRAPIE project, also the daily maximum 1-hour mean
385 concentration for NO_x is calculated. Maximum and minimum concentration difference are also
386 extracted and stored in a separate file, together with their position in the modelling domain and
387 the time of occurrence.

388 In summary, Module 3 provides the following output in separate text files:

- 389 1-hr and 24-hr average concentration difference of NO_x, $PM_{2.5}$ and PM_{10} over the selected
- 390 period (e.g. "nox_avg_tot_1.dat" or "nox_avg_tot_24.dat");
- 391 daily maximum 1-hour mean concentration difference of NO_x over the selected period
- 392 ("nox_dmm_tot.dat");
- 393 maximum and minimum concentration differences, with related position in the modelling
- 394 domain and time of occurrence (e.g. "nox_minpos.dat").

395 These output files can be visualized directly in a map viewer software like SURFER of similar; or
396 they can be transferred to the final module calculating the delta-external costs.

397

398 2.2.5 Module 4 - Calculation of delta-external costs (extern.m)

399 Module 4 represents the core of DIDEM integrated model. This script reads the average
400 concentration difference files provided by Module 3 and calculates the delta-external costs
401 associated to delta-concentrations.

402 The delta-external costs are calculated for each cell of the modelling domain r and for each
403 pollutant-outcome pair i (Table 1) with Equation 1, as described in Chapter 2.1.

404 The user is first asked to introduce the country of reference. For each pollutant-outcome pair, the
405 script reads the background rates n_i and the number of exposed individuals $p_{tot,i}$ from WHO
406 mortality and morbidity database. The code is organized to extract the most recent available data.
407 If no data is available for the selected country, an error message is displayed, and the user is asked
408 to change the reference country. The values of relative risk RR_i provided by HRAPIE project
409 recommendations, for each pollutant-outcome pair, are already implemented into the model. In
410 this way, the slope of the CRF for each pollutant-outcome pair can be calculated with Equation 2.

411 The number of exposed individuals (p_r in Equation 1) must be introduced by the user in form of
412 grid, with the same format of delta-concentration files. For an environmental analysis at the local
413 scale, this variable corresponds to the distribution of population over the modelling domain. It can
414 usually be calculated with the advice of GIS data and software. Monetary values per case of health
415 impact (mi in Equation 1) of EU countries (or Regions) are implemented in the model. These data
416 were taken by the most recent updates issued for the EU Clean Air Package (Holland, 2014b, Table
417 2). Monetary values are converted to the reference year using an average EU inflation rate of 2.1%
418 (Eurostat).

419 The range of overall delta-external costs is calculated following the recommendations on level of
420 confidence and additional effects, that is simulating Setting 1 and Setting 2 and their estimation of
421 uncertainties (cf. Chapter 2.1). Module 4 provides therefore two kinds of output:

- 422 a grid of delta-external costs distribution over the modelling domain;
- 423 two tables of overall delta-external costs, one for simulation setting, including mean values
- 424 and uncertainty range.

425

426 2.3 Case study

427 The DIDEM model was employed to a real case study, represented by a comparative analysis on
428 the district heating network of Turin, a town located in north-western Italy. District heating (DH) is

429 a technology used for supplying a town district or a complete town with the heat generated in
430 large production plants. District heating through combined heat and power (CHP) systems is an
431 increasingly popular solution to meet the thermal energy needs in urban areas (Lund and Van
432 Mathiesen, 2015).
433 The residential volume currently served by Turin's DH network amounts to about 59,76 million m^3.
434 The length of the network amounts to around 527 km of pipelines and is one of the most
435 extended in Europe (Figure 4). For more information about the actual network structure and
436 operating mode, refer to Jarre et al. (2016). Due to the persistence of critical concentration values
437 of pollutants in the air of Turin, local administrations have for some years been exploring the
438 possibility of obtaining an environmental benefit through the further extension of the DH network.
439 The results of the environmental analysis of this potential extension are reported in a study by
440 Ravina et al. (2017).
441 In the present case study, the analysis was performed comparing the present situation with an
442 alternative scenario. The present situation is represented by the actual environmental impacts of
443 the entire DH system. The alternative scenario is represented by a total absence of DH network,
444 where centralized autonomous boilers are used for household heating and sanitary hot water
445 production.
446 NO_x, and PM emissions were studied for a 1-year period. The latest available (related to 2016)
447 power units' emission flow rates were used in this study. The meteorological input datasets
448 collected in 2010 were used, since sufficiently accurate and complete datasets were not available
449 for 2016. However, average meteorological conditions in the period 2010-2016 in the studied area
450 were quite similar, so the introduced approximation is negligible. The emission flows and the
451 meteorological data had an hourly frequency.
452 Geophysical and meteorological data input in CALPUFF were obtained from the Regional Agency
453 for Environmental Protection of the Piedmont Region (ARPA). Weather and orographic data
454 covered a domain of 100 × 100 km^2 with a horizontal resolution of 1000 m. The same grid
455 represented also the modelling domain. For more information about input datasets and CALPUFF
456 model settings, refer to Ravina et al. (2017).
457 In the following, the two energy scenarios are described.
458
459 2.3.1 Actual situation
460 The present scenario is represented by Turin's DH system at its actual state of development. The
461 DH network is currently powered by a system of three large cogeneration combined cycle plants
462 fuelled by natural gas. A set of four integration and reserve boilers completes the system.
463 Information on nominal power and geometric configuration of the stacks are reported in Table 3.
464 Total energy production, NO_x emission and total suspended particulate (TSP) emission for the year
465 2016 were provided by the plants' operator IREN ENERGIA (IREN) and are reported in Table 4.
466 Hourly data of thermal energy transferred to the DH network and hourly emission flow rates of
467 NO_x were also provided by the plant operator. Thermal energy losses of the network amount to
468 353 GWh (16,3% of the net production). PM emission flow was calculated distributing the yearly
469 total PM amount on an hourly basis, scaling it to the hourly thermal energy production. Since
470 these plants are fuelled by natural gas, total particulate is expected to be composed mainly by fine
471 and ultra-fine components (Chang et al., 2004; D'Anna, 2009). For this reason, $PM_{2.5}$ and PM_{10}
472 emission flows were supposed equal to total PM emission flow. For the combined-cycle
473 cogeneration plants (Torino Nord and Moncalieri units), jointly producing heat and electricity, it
474 was not possible to allocate the amount of NO_x and PM attributable to the only thermal energy
475 transferred to the DH network. For this reason, the total flow of pollutant was used in the

476 simulations. For the simulation of pollutant dispersion, a point source was assigned to each plant.
477 The location of the emission sources is reported in Figure 4.
478
479 2.3.2 Alternative scenario
480 The alternative scenario was developed considering the absence of a DH network. Flow of thermal
481 energy, NO_x and total PM from the same areas currently served by the DH network were
482 calculated. In this scenario, thermal energy for household heating and production of sanitary hot
483 water was assumed to be provided by autonomous centralized boilers (one boiler per building).
484 The average rate of fuels distribution was assumed as: natural gas, 92.7%; diesel oil, 6.4%, heavy
485 fuel oil, 0.8%; LPG, 0.1%.
486 The annual thermal energy demand of the residential units was calculated with the model
487 proposed by Fracastoro and Serraino (2011). The annual amount was then distributed on an
488 hourly basis scaling it to the reference curve of a benchmark building subject to continuous
489 monitoring of consumption.
490 NO_x and TSP emission flow rates were calculated multiplying the hourly thermal energy
491 consumption by the corresponding emission factor. NO_x emission factor was set to 120 kg/GWh,
492 as established by Piedmont's Regional Decree n. 46-11968 (Piedmont Region, 2009). Total PM
493 emission factor was set to 4.3 kg/GWh according to EMEP/EEA database (EMEP/EEA, 2016). A
494 comparison between the total amount of thermal energy consumption, NO_x and total PM
495 emission of present and alternative scenario is reported in Table 4 and Table 5.
496 For the simulation of pollutants dispersion, the studied area was divided into 14 sub-areas based
497 on geometric criteria, to obtain a full coverage of the territory. A barycentric stack was assigned to
498 each sub-area. The location of the barycentric stacks is reported in Figure 4. The height of the
499 emission sources was set to 25 m, according to the average conformation of buildings that is
500 observed in this town (5 to 8 floors). The diameter of the emission sources was set to 0.8 m,
501 according to the standard sizing of centralized residential heating devices' chimneys (Taraschi and
502 Martinetto, 2015). The exhaust gas exit temperature and velocity were set to 363 K and 5.0 m/s
503 respectively.
504
505   3. Case study results
506 The DIDEM model was executed to simulate Turin's DH network case study. The simulation period
507 covered the entire heating season of year 2016, i.e. from January 1st to March 15th and from
508 October 15th to December 31st. The analysis of power plants emission data performed by Module
509 1 reported no missing or out-of-range values. Module 2 executed CALPUFF for present and
510 alternative scenario. The result provided by running Module 3 is reported in Figures 5 and 6. The
511 map of average 1-hour NO_x concentration difference over the metropolitan area of Turin is
512 reported in Figure 5. This map shows negative concentration differences, meaning that the
513 present situation (large centralized cogeneration plants and DH network) is preferable to the
514 alternative scenario (de-centralized autonomous heating of buildings). The reduction of NO_x
515 concentration ranges from 0.5 to $\mu g/m^3$ to 8.5 $\mu g/m^3$. These local effects are mainly limited to the
516 urban area and to the hilly areas located in the eastern part of the town. The map of average 1-
517 hour total PM concentration difference is reported in Figure 6. The concentration differences
518 reported in Figure 6 are still negative and range from -0.01 $\mu g/m^3$ to -0.3 $\mu g/m^3$. Lower values of
519 total PM concentration with respect to NO_x are the result of lower emission flows and lower
520 emission factors (Table 4 and Table 5).
521 Delta-external costs were calculated running Module 4. The delta-external costs distribution over
522 the entire modelling domain are reported in Figure 7. The area with the highest external costs

523   reduction corresponds to the urban centre of Turin. A higher reduction of external costs is the
524   result of a higher concentration difference matched to a high population density.

525   Total delta-external costs for the case study are reported in Table 6. Table 6 reports the results of
526   Setting 1 and Setting 2 and the related maximum and minimum values. If pollutant-outcome pairs
527   with high confidence level on CRF data are considered (Setting 1), total external costs reduction
528   ranges from 3,880,000 €/y to 12,245,000 €/y, with a mean value of 8,550,000 €/y. If pollutant-
529   outcome pairs with both high and medium confidence level on CRF data are considered (Setting 2),
530   total external costs reduction ranges from 32,245,000 €/y to 85,652,000 €/y, with a mean value of
531   58,815,000 €/y. If the same result is reported in term of delta-external cost per unit of net thermal
532   energy consumption (€/kWh), the obtained value ranges from -0.214 $€_{cent}$/kWh to -4.724
533    $€_{cent}$/kWh.

534   The results reported in Figure 7 and Table 6 show that the reduction of environmental impacts (i.e.
535   lower NO_x and PM concentration) brought by the presence Turin's DH network corresponds to a
536   significant reduction of external health costs. Without a DH network, Turin would have been more
537   polluted, and local collective health care costs would have been significantly higher. Figure 8
538   reports total delta-external costs divided by pollutant and exposure term (short and long term
539   exposure), for Setting 1 and Setting 2 respectively. If Setting 1 is considered, the largest
540   contribution to delta-external costs is given by short-term exposure to NO_2 (81.9%). If Setting 2 is
541   considered, the largest contribution is given by long-term exposure to NO_2 (67%). It is important to
542   note that the importance of PM impact is higher if delta-external costs are analysed instead of
543   delta-concentrations. In fact, even though the reduction of total PM concentration is one order of
544   magnitude smaller than NO_x reduction, the contribution of PM pollution to total delta-external
545   costs is around 12 % – 18%. This is due to the higher values of relative risk associated to the CRFs
546   of PM.

547

548   4.   Discussion

549   A comparison of the case study results with other publications provides information on DIDEM
550   model performance. Several studies are reported in bibliography where external costs of energy
551   systems are calculated with the use of modelling tools. Bachmann and Van der Kamp (2014)
552   applied the EcoSenseWeb model to the case of a DeNOx retrofit at a coal-fired power plant
553   hypothetically located at three different sites in Europe. The external costs of the plant without a
554   DeNOx ranged between 2.30 $€_{cent}$/kWh$_{el}$ and 4.15 $€_{cent}$/kWh$_{el}$. The installation of a DeNOx
555   provided a reduction of marginal external costs of 33%, 22% and 17% respectively, depending on
556   the location of the plant.

557   Andersen et al. (2006). compared the performance of EVA and EcoSense models on three
558   combined heat and power (CHP) plants in Denmark: a CHP unit fuelled by coal (60%) and natural
559   gas (40%), a CHP unit fuelled by coal only, and a waste incinerator. The three plants emitted an
560   average of 147 t, 14 t and 6.3 t of primary $PM_{2.5}$ respectively. The EVA model returned a value of
561   external costs per unit of kWh$_t$ (year 2005) of 1.32 $€_{cent}$/kWh$_t$, 0.24 $€_{cent}$/kWh$_t$, 4.45 $€_{cent}$/kWh$_t$
562   respectively. The same calculation done with Ecosense model resulted in significantly lower values
563   (around 40%).

564   Saez et al. (1998) analysed the effect that the consideration of external costs may have on biomass
565   energy competitiveness. EcoSense model was applied to a 20 MW power plant located in
566   Southern Spain, fuelled with an herbaceous energy crop. The only contribution of $PM_{2.5}$ was
567   considered to contribute to total health external costs. The results showed a unitary external cost
568   between 0.28 €/kWh and 0.67 €/kWh.

569   Van der Kamp and Bachmann (2015) calculated external costs on a 600 MW$_{el}$ pulverized coal
570   combustion unit located in Western France. Four methodologies of implementation of the impact

571 pathway approach were compared: ExternE1998 (ExternE), New Elements for the Assessment of
572 External Costs from Energy Technologies (NewExt2004, European Commission 2004), New Energy
573 Externalities Developments for Sustainability (NEEDS2009) and a new version of EcoSenseWeb
574 updated with the latest WHO recommendations (Year2013). This study provided the following unit
575 external costs: ExternE1998, 5.21 €$_{cent2000}$/kWh$_{el}$; NewExt2004, 1.77 €$_{cent2000}$/kWh$_{el}$; NEEDS2009,
576 2.78 €$_{cent2000}$/kWh$_{el}$; Year2013, 3.21 €$_{cent2000}$/kWh$_{el}$.

577 Comparing the performance of DIDEM model with existing studies, it can be concluded that the
578 result is consistent with the average values commonly found in the literature. On the other hand,
579 these results cannot be generalized, because they depend on the emission profile and location of
580 the source. More information could be obtained by simulating the same case study with another
581 modelling tool.

582 Beside the considerations on modelling results, some important comments can be obtained by
583 comparing DIDEM model's structure and scope with existing methodologies and tools. Anenberg
584 et al. (2016) recently published a review article that was first developed as a white paper for input
585 to the WHO expert meeting on Health Risk Assessment held in Bonn, Germany, May 12-13, 2014.
586 In this article, 12 multinational air pollution health impact assessment tools were analysed and
587 compared. The paper confirms that the quantification and minimization of uncertainty remains
588 the main challenge in external health costs analysis. The impact pathway approach combines in
589 fact information from different sources such as pollutant exposure, population data, and CRFs.
590 Each of these source carries with it some degree of uncertainty, that has an influence on the result.
591 If the air quality modelling approach is considered, two main kinds of modelling tools can be
592 identified: detailed air quality models or reduced form models. Detailed air quality models account
593 for the complex atmospheric chemistry and transport governing air pollution, and may be
594 implemented for analysis at the local scale. Since it implements CALPUFF's detailed structure, the
595 DIDEM model can be classified in this category. Other examples include the Ecosense model
596 (Preiss and Klotz, 2008; IER, 2004) or the EVA model (Brandt et al., 2013; Andersen et al., 2006).
597 Ecosense uses the WTM-model (Windrose Trajectory Model; Derwent et al., 1988) for estimating
598 pollutant dispersion. The model assumes a constant average wind speed and the trajectories of
599 emission transport are assumed to run along straight lines. EVA implements a non-linear Eulerian
600 air pollution model, that comprises a standard local Gaussian plume model OML (Operational
601 Meteorological Air quality model; Olesen et. al., 1992) and the regional Eulerian model DEHM
602 (Danish Eulerian Hemispheric Model; Christensen, 1997; Frohn et al., 2001). Reduced form tools
603 use broad-scale estimates for air pollution impacts and are increasingly being used at a national
604 and regional scale, as they are less resource intensive and more flexible (Fann et al., 2012).
605 Examples of reduced form models are the Geographic Information System (GIS) based BenMAP
606 tool (Davidson et al., 2007; Sun et al., 2015), the TM5-FASST tool (van Dingenen et al., 2014), the
607 Long-range Energy Alternatives Planning System - Integrated Benefits Calculator (LEAP-IBC) tool
608 (Lazarus et al. 1995), or the Health Impact Assessment (HIA) model (Flachs et al., 2012, Flachs et
609 al., 2013).

610 Detailed air quality models like the DIDEM model, since are based on advanced simulation of
611 dispersion phenomena (e.g. non-stationary processes, fine spatial resolution and chemical
612 transformation, cf. Paragraph 2.1.1), have the main advantage of reducing the amount of
613 uncertainty associated with the dispersion modelling step.

614 This is an important contribution, since the uncertainty related to air modelling has been
615 calculated to contribute in a significant amount to the overall error (Bridges et al., 2015; van der
616 Kamp and Bachmann, 2015). Reduced form models may, in some case, not capture the full scope
617 of changes in ambient air pollution, because the treatment of secondary formation, transport, and
618 deposition is simplified (Fann et al., 2012).

619 Anyway, the use of detailed air quality modelling also presents some disadvantage. The first is that
620 their use is resource-consuming (a complete CALPUFF run of the case study scenarios took around
621 16 hours). Another disadvantage is that modelled concentrations may not match the method or
622 spatial resolution of the exposure characterization in the epidemiology studies from which
623 concentration-response associations are drawn, which may introduce error into the analysis
624 (Anenberg et al., 2016).

625 Beside the air modelling approach, another main source of uncertainty in modelling external
626 health impacts and costs is related to the simulation of exposure-response-monetary evaluation
627 steps. The main sources of errors in these steps are: the definition of the CRFs, the estimation of
628 exposure, the extrapolation of baseline mortality and morbidity rates and the definition of
629 monetary values. The DIDEM model is based on latest WHO recommendations on air pollution
630 health impacts, resulted by the REVIHAAP and HRAPIE projects (WHO, 2013a; WHO, 2013b). These
631 advices are based on a review of the latest scientific evidence on the health effects of pollutants.
632 The methodology reported in the HRAPIE project incorporates a sensitivity analysis by
633 including/excluding a limited set of parameters. In addition, an indication of the confidence
634 intervals around the values of relative risk of each pollutant-outcome association is provided.
635 These aspects favour the quantification and reduction of the overall uncertainty.

636 If the features of usability and flexibility are considered, the DIDEM model is flexible enough to
637 allow users to input their own data sets (emission flows, background mortality and morbidity rates,
638 population data). On the other hand, its usability is limited by two factors: the need of expertise in
639 setting up CALPUFF model pre-processing, and the absence of a graphical user's interface (GUI).

640 Resuming the conclusion reported by Anenberg et al. (2016), different tools are appropriate for
641 different assessment contexts, and analysis must consider the technical and operational
642 specifications of the tool necessary to meet the needs of the assessment context. The DIDEM
643 model appears to be a suitable tool for cost-benefit comparative analysis at the local scale. It
644 should be tested on different new scenarios and case studies, to achieve more information on its
645 performance and usability. The comparison with other similar modelling tools may contribute to
646 this perspective.

647 A possible improvement of the DIDEM model could consist in enlarging the scope of analysis.
648 Other factors than the sole emission from power units could be implemented in the model, to
649 allow a wider assessment context. Some examples reported in bibliography include the calculation
650 of external health costs in transport scenarios (Miranda et al., 2016) or refurbishment and other
651 heat saving measures on buildings (Zvingilaite and Jacobsen, 2015).

652

653   5. Conclusion

654 External costs are a direct indicator of air pollution impacts on human health. Their quantification
655 provides clear and detailed information, suitable to be used at all communication levels
656 (companies, administrations, population). Comparative analysis is an efficient method for
657 evaluating different solutions and support policy and strategic decision. Modelling tools have been
658 widely used to implement the estimation of externalities associated to air pollution and they are
659 increasingly integrated into decision processes. This paper presented the DIATI Dispersion and
660 Externalities (DIDEM) model, that was developed at the Department of Engineering for
661 Environment, Land and Infrastructures of Turin Polytechnic, Italy. DIDEM integrates CALPUFF
662 dispersion modelling with latest recommendations on health concentration-response functions
663 issued by the WHO, and latest updates of monetary values elaborated for the EU Clean Air Policy
664 Package.

665 The DIDEM model was designed with a regional scope (Europe) to perform comparative analysis at
666 the local scale. Compared to other existing modelling tools, DIDEM allows a detailed spatial

667 resolution (down to 1000 m) and enough flexibility in the definition of the pollution source and
668 background exposure data. An estimation of uncertainty is provided with the estimation of health
669 impacts, to include in the analysis those pollutant-health outcome pairs whose data are currently
670 subject to a medium confidence level. The application of DIDEM model could, therefore, be
671 preferable to the use of a reduced form model in some circumstances (at the town scale, for
672 example). On the other hand, the main drawback is that the use of CALPUFF model and a limited
673 interface, require users with a high level of expertise as well as higher calculation resources.
674 In summary, the application of DIDEM model is recommended for the analysis of the health
675 effects of local emission scenarios (up to 100-200 km of domain extension), where detailed
676 information about the emission sources (type and location of source, hourly emission flows,
677 detailed emission parameters) and background exposure to health effects is available. Users must
678 be confident with CALPUFF or other similar dispersion models. Conversely, DIDEM model is not
679 recommendable for the analysis at the national or regional scale working with wider spatial
680 resolution and aggregated emission data (e.g. for the development of national or regional policies).
681 Different tools are appropriate for different assessment contexts. The development of high-
682 resolution tools based on detailed air quality modelling, like DIDEM, allow for greater confidence
683 and precision of the results. Nevertheless, to quantify and limit the overall uncertainty of the
684 simulation chain, a great effort is still needed in the definition of more detailed, harmonized and
685 widespread datasets (e.g. local baseline mortality and morbidity rates), exposure-response
686 functions (e.g. local epidemiological studies) and monetary evaluation (e.g. local socio-economic
687 studies).
688

689 **Conflict of interest**
690 The authors declare that they have no conflict of interest.
691

692 **Acknowledge**
693 The authors would like to acknowledge IREN ENERGIA S.p.A. company for the data supplied and
694 for their continuous support in the development of this work.
695

696 **References**
697 Andersen M.S., Frohn L.M., Nielsen J.S., Nielsen M., Jensen J.B., Jensen S.S., Christensen J., Brandt
698 J. (2006), EVA – a non-linear eulerian approach for assessment of health-cost externalities of air
699 pollution. Paper presented at the Biennial Conference of the International Society for Ecological
700 Economics (ISEE), New Delhi, December 2006. Department of Environmental Science, Aarhus
701 University, Denmark;

702

703 Anenberg S.C., Belova A., Bramdt J., Fann N., Greco S., Guttikunda S., Heroux M.E., Hurley F.,
704 Krzyzanowski M., Medina S., Miller B., Pandey K., Roos J., Van Dingenen R. (2016), Survey of
705 Ambient Air Pollution Health Risk Assessment Tools, Risk Analysis, 36 (9), 1718 – 1736; DOI:
706 10.1111/risa.12540

707

708 Anenberg S.C., Horowitz L.W., Tong D.Q., West J.J. (2010), An estimate of the global burden of
709 anthropogenic ozone and fine particulate matter on premature human mortality using
710 atmospheric modeling. Environmental Health Perspectives, 2010; 118(9):1189–1195; DOI:
711 10.1289/ehp.0901220
712

713 Anenberg S.C., West J.J., Fiore A.M., Jaffe D.A., Prather M.J., Bergmann D., Cuvelier K., Dentener
714 F.J., Duncan B.N., Gauss M., Hess P., Jonson J.E., Lupu A., MacKenzie I.A., Marmer E., Park R.J.,
715 Sanderson M.G., Schultz M., Shindell D.T., Szopa S., Vivanco M.G., Wild O., Zeng G.
716 Intercontinental impacts of ozone pollution on human mortality. Environmental Science &
717 Technology, 2009; 43:6482–6487; DOI: 10.1021/es900518z
718
719 Amann M. (2013), Policy scenarios for the revision of the Thematic Strategy on Air Pollution. TSAP
720 Report #10. Laxenburg, Austria: International Institute for Applied Systems Analysis;
721
722 Bachmann T.M., van der Kamp J. (2014), Environmental cost-benefit analysis and the EU
723 (European Union) Industrial Emissions Directive: exploring the societal efficiency of a DeNOx
724 retrofit at a coal-fired power plant, Energy, 68:125-139. DOI:
725 http://dx.doi.org/10.1016/j.energy.2014.02.051
726
727 Blengini G.A., Brizio E., Cibrario M., Genon G. (2011), LCA of bioenergy chains in Piedmont (Italy): a
728 case study to support public decision makers towards sustainability, Biomass Bioenergy, 57, 36-47;
729 DOI: https://doi.org/10.1016/j.resconrec.2011.10.003
730
731 Brandt J., Silver J. D., Christensen J. H., Andersen M. S., Bønløkke J. H., Sigsgaard T., Geels C., Gross
732 A., Hansen A.B., Hansen K. M., Hedegaard G. B., Kaas E., Frohn L.M. (2013), Contribution from the
733 ten major emission sectors in Europe and Denmark to the health-cost externalities of air pollution
734 using the EVA model system – an integrated modelling approach, Atmos. Chem. Phys., 13: 7725–
735 7746; DOI:10.5194/acp-13-7725-2013
736
737 Bridges A., Felder F.A., McKelvey K., Niyogi I. (2015), Uncertainty in energy planning: Estimating
738 the health impacts of air pollution from fossil fuel electricity generation, Energy Research & Social
739 Science, 6:74–77; DOI: http://dx.doi.org/10.1016/j.erss.2014.12.002
740
741 Chambliss S.E., Silva R., West J.J., Zeinali M., Minjares R. (2014), Estimating source-attributable
742 health impacts of ambient fine particulate matter exposure: Global premature mortality from
743 surface transportation emissions in 2005. Environmental Research Letters, 9:104-109; DOI:
744 https://doi.org/10.1088/1748-9326/9/10/104009
745
746 Chang M.C.O., Chow J.C., Watson J.G., Hopke P.K., Seung-Muk Y., England G.C. (2004),
747 Measurement of ultrafine particle size distributions from coal-, oil-, and gas-fired stationary
748 combustion sources, Journal of the Air & Waste Management Association, 54:12, 1494-1505, DOI:
749 10.1080/10473289.2004.10471010
750
751 Christensen J.H., (1997), The Danish Eulerian Hemispheric Model – A three-dimensional air
752 pollution model used for the Arctic, Atmospheric Environment, 31:4169-4191.
753
754 Cohen A.J., Anderson H.R., Ostro B., Pandey K.D., Krzyzanowski M., Kunzli N., Gutschmidt K., Pope
755 C.A. III, Romieu I., Samet J.M., Smith K.R. (2004), Urban air pollution, pp. 1353–1434 in Ezzati M.,
756 Lopez A.D., Rodgers A., Murray C.J.L. (eds). Comparative Quantification of Health Risks: Global and
757 Regional Burden of Disease Due to Selected Major Risk Factors. Geneva: World Health
758 Organization;

759

760 Davidson K., Hallberg A., McCubbin D., Hubbell B. (2007), Analysis of $PM_{2.5}$ using the
761 environmental benefits mapping and analysis program (BenMAP), Journal of Toxicology and
762 Environmental Health, Part A, 70:3-4, 332-346; DOI:10.1080/15287390600884982

763

764 Derwent R.G., Dollard G.J., Metcalfe S.E. (1988), On the nitrogen budget for the United Kingdom
765 and north-west Europe, Q.J.R. Meteorol. Soc., 114:1127-1152

766

767 van Dingenen R., Leitao J., Dentener F. (2014), A multi-metric global source-receptor model for
768 integrated impact assessment of climate and air quality policy scenarios. Geophysical Research
769 Abstracts, Vol. 16, EGU2014-13949, 2014.

770

771 D'Anna A. (2009), Combustion-formed nanoparticles- Proceedings of the Combustion Institute 32,
772 593–613.

773

774 EMEP/EEA (2016), Air pollutant emission inventory guidebook. EEA Technical report. ISSN 1725–
775 2237. Technical guidance to prepare national emission inventories.

776

777 European Commission (1995), Externalities of Energy - Vol. 2: Methodology - method for
778 estimation of physical impacts and monetary valuation for priority impact pathways. European
779 Commission DG XII "Science, Research and Development", JOULE, Luxembourg.

780

781 European Commission (2004), New Elements for the Assessment of External Costs from Energy
782 Technologies (NewExt) - Final Report to the European Commission, DG Research, Technological
783 Development and Demonstration (RTD); European Commission, Brussels, p 333;

784

785 European Commission (2005), ExternE - Externalities of Energy: Methodology 2005 update. Office
786 for Official Publication of the European Communities, Luxembourg.

787

788 Eurostat, Harmonized Indices of Consumer Prices (HICP) - main tables.
789 http://ec.europa.eu/eurostat/web/hicp/data/main-tables (accessed September 7, 2017).

790

791 Fann N., Lamson A.D., Anenberg S.C., Wesson K., Risley D., Hubbell B.J., (2011), Estimating the
792 national public health burden associated with $PM_{2.5}$ and ozone. Risk Analysis, 32(1):81– 95; DOI:
793 10.1111/j.1539-6924.2011.01630.x

794

795 Fann N., Baker K.R., Fulcher C.M. (2012), Characterizing the $PM_{2.5}$-related health benefits of
796 emission reductions for 17 industrial, area and mobile emission sectors across the U.S., Environ.
797 Int., 49:141–51. DOI: https://doi.org/10.1016/j.envint.2012.08.017

798

799 Flachs E. M., Bønløkke J.H., Sigsgaard T. (2012), Description of the HIA line in the CEEH integrated
800 modelling chain, CEEH Scientific Report No. 5, Centre for Energy, Environment and Health (CEEH),
801 2012.

802

803 Flachs E.M., Sørensen J., Bønløkke J.H., Brønnum-Hansen H. (2013), Population dynamics and air
804 pollution: the impact of demographics on health impact assessment of air pollution, Journal of

805 Environmental and Public Health, Volume 2013, Article ID 760259, 12 p.; DOI:
806 http://dx.doi.org/10.1155/2013/760259
807

808 Fracastoro G.V., Serraino M. (2011), A methodology for assessing the energy performance of large
809 scale building stocks and possible applications. Energy and Buildings, 43:844–852; DOI:
810 https://doi.org/10.1016/j.enbuild.2010.12.004
811

812 Frohn L.M., Christensen J.H., Brandt J., Hertel O. (2001), Development of a high resolution
813 integrated nested model for studying air pollution in Denmark, Physics and Chemistry of the Earth,
814 26:10, 769-774.
815

816 Gehring U., Pattenden S., Slachtova H., Antovae T., Braun-Fahrlander C., Fabianova E., Fletcher T.,
817 Galassi C., Hoek G., Kuzmin S.V., Luttmann- Gibson H., Moshammeree H., Rudnai P., Zlotkowska R.,
818 Heinrich J. (2006), Parental education and children's respiratory and allergic symptoms in the
819 Pollution and the Young (PATY) study, Eur Respir J, 27: 95–107; DOI:
820 10.1183/09031936.06.00017205
821 Golden Software. Surfer®. http://www.goldensoftware.com/products/surfer (accessed November
822 3, 2017)
823

824 Guttikunda S.K., Jawahar P. (2012), Application of SIM-air modeling tools to assess air quality in
825 Indian cities. Atmospheric Environment, 62:551–561;
826 https://doi.org/10.1016/j.atmosenv.2012.08.074
827

828 He K., Lei Y., Pan X., Zhang Y, Zhang Q, Chen D. (2010), Co-benefits from energy policies in China.
829 Energy, 35(11):4265-4272; DOI: https://doi.org/10.1016/j.energy.2008.07.021
830

831 Holland M., Hunt A., Hurley F., Navrud S., Watkiss P. (2005), Service contract for carrying out cost-
832 benefit analysis of air quality related issues, in particular in the Clean Air for Europe (CAFE)
833 Programme. Methodology for the cost-benefit analysis for CAFE: Volume 1: Overview of
834 methodology. Web published:AEATechnology Environment, available at:
835 http://europa.eu.int/comm/environment/air/cafe/activities/cba. htm.
836

837 Holland, M. (2014a), Cost-benefit analysis of final policy scenarios for the EU Clean Air Package -
838 Version 2, corresponding to IIASA TSAP Report 11, Version 1. UK, EMRC.
839

840 Holland M. (2014b), Cost-Benefit Analysis of Final Policy Scenarios for the EU Clean Air Package -
841 Version 2, Corresponding to IIASA TSAP Report 11, Version 2a. EMRC.
842

843 Hubbell B.J., Hallberg A., McCubbin D., Post E. (2005), Health-related benefits of attaining the 8-hr
844 ozone standard. Environmental Health Perspective, 113(1):73–82; DOI: 10.1289/ehp.7186
845

846 IER (2004), EcoSense 4.0 User's Manual, Institute of Energy Economics and the Rational Use of
847 Energy, University of Stuttgart, p54;

848

849 Iren Energia company website. http://www.irenenergia.it/. (accessed September 7, 2017).
850

851 Jarre M., Noussan M., Poggio A. (2016), Operational analysis of natural gas combined cycle CHP
852 plants: energy performance and pollutant emissions, Appl. Therm. Eng., 100:304–314; DOI:
853 https://doi.org/10.1016/j.applthermaleng.2016.02.040
854
855 van der Kamp J., Bachmann T.M. (2015), Health-related external cost assessment in Europe:
856 methodological developments from ExternE to the 2013 Clean Air Policy Package. Environ. Sci.
857 Technol. 49, 2929–2938; DOI: 10.1021/es5054607
858
859 Kampa M., Castanas E. (2008), Human health effects of air pollution, Environmental Pollution 151,
860 362-367; DOI: https://doi.org/10.1016/j.envpol.2007.06.012
861
862 Kheirbeck I., Wheeler K., Walters S., Kass D., Matte T. (2013), $PM_{2.5}$ and ozone health impacts and
863 disparities in New York City: Sensitivity to spatial and temporal resolution. Air Quality Atmosphere
864 and Health, 6(2):473–486;
865
866 Kirtman B., Power S.B., Adedoyin A.J., Boer G.J., Bojariu R., Camilloni I., Doblas- Reyes I., Fiore A.M.,
867 Kimoto M., Meehl G., Prather M., Sarr A., Schar C., Sutton R., van Oldenborgh G.J., Vecchi G.,
868 Wang H.-J. (2013), Near-term climate change: projections and predictability. In: Plattner G.K.,
869 Tignor M., Allen S.K., Boschung J.,
870
871 Lai C.K., Beasley R., Crane J., Foliaki S., Shah J., Weiland S. (2009). Global variation in the
872 prevalence and severity of asthma symptoms: phase three of the International Study of Asthma
873 and Allergies in Childhood (ISAAC), Thorax, 64(6):476–483. DOI: 10.1136/thx.2008.106609
874
875 Lazarus M., Von Hippel D., Hill D., Margolis R. (1995), A guide to environmental analysis for energy
876 planners. companion manual to assist users of LEAP. Stockholm Environment Institute, Boston,
877 MA, USA
878
879 Likhvar V.N., Pascal M., Markakis K., Colette A., Hauglaustaine D. (2015), A multi-scale health
880 impact assessment of air pollution over the 21st century. Science of the Total Environment;
881 514:439–449; DOI: https://doi.org/10.1016/j.scitotenv.2015.02.002
882
883 Lim S.S., Vos T., Flaxman A.D., Danaei G., Shibuya K., Adair- Rohani H., A comparative risk
884 assessment of burden of disease and injury attributable to 67 risk factors and risk factor clusters in
885 21 regions, 1990–2010: A systematic analysis for the Global Burden of Disease Study 2010. Lancet,
886 2013; 380(9859):2224–2260; DOI: https://doi.org/10.1016/S0140-6736(12)61766-8
887
888 Lund R., Van Mathiesen B. (2015), Large combined heat and power plants in sustainable energy
889 systems. Appl. Energy, 142:389–395; DOI: https://doi.org/10.1016/j.apenergy.2015.01.013
890
891 Mathworks Matlab® Software. https://it.mathworks.com/products/matlab.html (accessed
892 September 7, 2017)
893
894 McConnell R., Berhane K., Gilliland F., Molitor J., Thomas D., Lurmann F., Avol E., Gauderman W.J.,
895 Peters J.M. (2003), Prospective study of air pollution and bronchitic symptoms in children with
896 asthma. American Journal of Respiratory and Critical Care Medicine, 168(7):790–797; DOI:
897 https://doi.org/10.1164/rccm.200304-466OC
898

899 Miranda A.I., Ferreira J., Silveira C., Relvas H., Duque L., Roebeling P., Lopes M., Costa S., Monteiro
900 A., Gama C. Sá E., Borregoa C., Teixeira J.P. (2016), A cost-efficiency and health benefit approach
901 to improve urban air quality, Science of the Total Environment, 569–570:342–351; DOI:
902 http://dx.doi.org/10.1016/j.scitotenv.2016.06.102
903
904 Nauels A., Xia Y., Bex V., Midgley P., Stocker T.F., Quin D. (Eds.), Climate Change 2013: The Physical
905 Science Basis. Conribution of Working Group I to the Fifth Assessment Report of the
906 Intergovernmental Panel on Climate Change. Cambridge University Press, Cambridge, UK and New
907 York, NY, USA.
908
909 Nawadha A. (2013), Reductions of $PM_{2.5}$ air concentrations and possible effects on premature
910 mortality in Japan. Water, Air, & Soil Pollution, 224:1508;
911
912 NEEDS2009 - New Energy Externalities Developments for Sustainability. http://esu-
913 services.ch/data/needs/ (accessed September 7, 2017).
914
915 Olesen H.R., Løfstrøm P., Berkowicz R. and Jensen A.B. (1992), An Improved Dispersion Model for
916 Regulatory Use - The OML Model, pp. 29-38 in Dop H. van and Kallos G.: Air Pollution Modelling
917 and Its Applications IX, Plenum Press.
918
919 Ostro, B.D., Rothschild, S. (1989), Air pollution and acute respiratory morbidity: an observational
920 study of multiple pollutants. Environmental Research, 50:238–247.
921
922 Panepinto D., Brizio E., Genon G. (2014), Atmospheric pollutants and air quality effects: limitation
923 costs and environmental advantages (a cost–benefit approach), Clean Techn Environ Policy,
924 16:1805–1813; DOI 10.1007/s10098-014-0727-6
925
926 Piedmont Region (2009), Decree of the Regional Council of 4 August 2009, no. 46-11968. Update
927 of the Regional Plan for the Rehabilitation and Protection of Air Quality - Draft plan for
928 environmental heating and conditioning and implementing provisions on energy performance in
929 construction pursuant to Article 21, paragraph 1, letters a) b) q) of Regional Law 28 May 2007, no.
930 13. In Italian.
931
932 Preiss P., Klotz, V. (2008), EcoSenseWeb V1.3 User's Manual and description of updated and
933 extended draft tools for the detailed site dependent assessment of external sosts. Institute of
934 Energy Economics and the Rational Use of Energy (IER), University of Stuttgart, Germany, p 63;

935
936 QGIS open source software. https://www.qgis.org/it/site/ (accessed November 3, 2017)
937
938 Rabl A., Spadaro J.V. (1999), Damages and costs of air pollution: an analysis of uncertainties.
939 Environ. Int. 25, 29–46.
940
941 Ravina M. (2016), Development and application of a comprehensive methodology for the analysis
942 of global and local emissions of energy systems. PhD Dissertation. Politecnico di Torino, Italy. DOI:
943 10.6092/polito/porto/2674649
944

945 Ravina M., Panepinto D., Zanetti M.C., Genon G. (2017), Environmental analysis of a potential
946 district heating network powered by a large-scale cogeneration plant. Environ. Sci. Pollut. Res.,
947 24:13424–13436; DOI 10.1007/s11356-017-8863-2

949 Saez R.M., Linares P., Leal J. (1998), Assessment of the externalities of biomass energy, and a
950 comparison of its full costs with coal. Biomass and Bioenergy, 14:469-478;

952 Schindler C., Keidel D., Gerbase M.W., Zemp E., Bettschart R., Brandli O., Brutsche M.H., Burdet L.,
953 Karrer W., Knopfli B., Pons M., Rapp R., Bayer-Oglesby L., Kunzli N., Schwartz J., Liu L.-J.S.,
954 Ackermann-Liebrich U., Rochat T., The SAPALDIA Team (2009). Improvements in PM_{10} exposure
955 and reduced rates of respiratory symptoms in a cohort of Swiss adults (SAPALDIA). Am. J. Respir.
956 Crit. Care Med. 179, 579–587; DOI: https://doi.org/10.1164/rccm.200803-388OC

958 Sun J., Fu J.S., Huang K., Gao Y. (2015) Estimation of future $PM_{2.5}$- and ozone-related mortality
959 over the continental United States in a changing climate: An application of high-resolution
960 dynamical downscaling technique, Journal of the Air & Waste Management Association, 65:5, 611-
961 623; DOI: 10.1080/10962247.2015.1033068

963 Taraschi N., Martinetto M. (2015) Le canne fumarie. Grafill. 186 pp. ISBN: 88-8207-947-5. In Italian.

965 University of Stuttgart. Institute of Energy Economics and the Rational Use of Energy (IER). ExternE
966 - External Costs of Energy. http://www.externe.info/ (accessed September 7, 2017).

968 U.S. Environmental Protection Agency (US EPA) (2011), CALPUFF modeling system user's manual,
969 version 6

971 U.S. Environmental Protection Agency (US EPA) (2012), Regulatory Impact Analysis for the Final
972 Revisions to the National Ambient Air Quality Standards for Particulate Matter. EPA- 452/R-12-005.
973 Washington, DC: U.S. Environmental Protection Agency;

975 Viggiano F., Panepinto D., Genon G. (2014 a) Energy from biomass: a contribution to GHG
976 limitation and sustainability of the local impact aspect, WIT Trans Ecol Environ, 190 (2), 1023-1034;
977 DOI: 10.2495/EQ140962

979 Viggiano F., Panepinto D., Genon G. (2014 b), The environmental compatibility of biomass plants: a
980 methodological approach, WIT Trans Ecol Environ, 181, 201-212; DO: 10.2495/EID140171

982 Wesson K, Fann N, Morris M, Fox T, Hubbell B. (2010), A multipollutant risk-based approach to air
983 quality management: Case study for Detroit. Atmospheric Pollution Research, 1:296–304; DOI:
984 https://doi.org/10.5094/APR.2010.037

986 WHO (2013a), Health Risks of Air Pollution in Europe - HRAPIE Project. Recommendations for
987 concentration–response functions for cost–benefit analysis of particulate matter, ozone and
988 nitrogen dioxide; World Health Organization, Regional Office for Europe, Copenaghen, Denmark; p
989 54.

991 WHO (2013b), Review of evidence on health aspects of air pollution – REVIHAAP Project. Technical
992 report; The WHO European Centre for Environment and Health, Bonn, Germany; p 302.

993

994 WHO HMDB. European Hospital Morbidity Database. World Health Organization Regional Office
995 for Europe. http://data.euro.who.int/hmdb/ (accessed September 7, 2017).

996

997 WHO HFA-DB, European health for all database (HFA-DB). World Health Organization Regional
998 Office for Europe. http://data.euro.who.int/hfadb/ (accessed September 7, 2017).

999

1000 Zvingilaite E., Jacobsen H.K. (2015), Heat savings and heat generation technologies: Modelling of
1001 residential investment behaviour with local health costs, Energy Policy, 77:31–45; DOI:
1002 http://dx.doi.org/10.1016/j.enpol.2014.11.032

1003
1004

1005 **List of Figures**
1006 Figure 1. Schematic representation of the impact pathway approach (adapted from Van der Kamp
1007 and Bachmann, 2015).

1008

1009 Figure 2. DIDEM model input and output.

1010

1011 Figure 3. DIDEM model structure. Schematic representation of input and output from each
1012 Module.

1013

1014 Figure 4. Present extension of Turin's DH network. Location of the plants powering the DH
1015 network. Location of the barycentric stacks assigned to the residential areas. The mesh grid
1016 represents the cells of the modelling domain.

1017

1018 Figure 5. Average 1-hour delta-concentration map of NO_x in the metropolitan area of Turin,
1019 resulting from CALPUFF simulation. Average is calculated over the entire heating season (October
1020 to March).

1021

1022 Figure 6. Average 1-hour delta-concentration map of total PM in the metropolitan area of Turin,
1023 resulting from CALPUFF simulation. Average is calculated over the entire heating season (October
1024 to March).

1025

1026 Figure 7. Map of average delta-external costs resulting from the integrated simulation with DIDEM
1027 model, referred to Setting 1.

1028

1029 Figure 8. Case study results. Contribution of pollutant (NO_2 and PM) and exposure term (short and
1030 long term exposure) to the total delta-external costs, for Setting 1 (a) and Setting 2 (b) respectively.

1031
1032

1033 **List of Tables**
1034 Table 1. List of the pollutant-outcome pairs implemented in the DIDEM model, with the relative
1035 category of confidence level, average relative risk of the CRF and source of background health data
1036 (modified from WHO 2013a).

1037

1038 Table 2. Monetary values implemented in the DIDEM model (from Holland, 2014b).

1039

1040 Table 3. Data on power plants and emission sources presently feeding the DH network in Turin,
1041 Italy

1042

1043 Table 4. Energy and pollutants emission balance for the case study considered, present scenario
1044 year 2016.
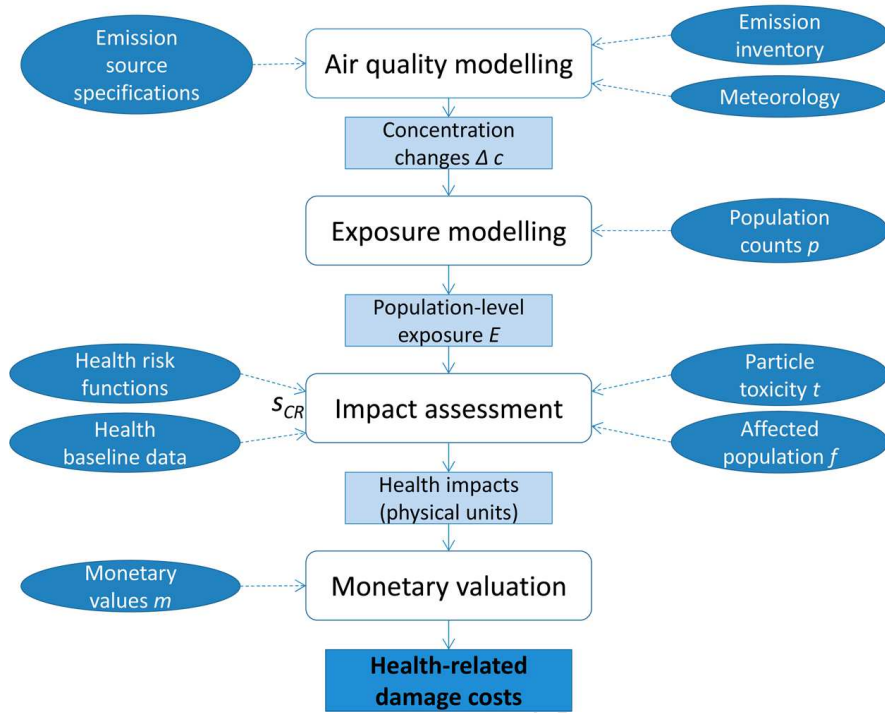
1045

1046 Table 5. Energy and pollutants emission balance for the case study considered, alternative
1047 scenario year 2016.

1048

1049 Table 6. Result of delta-external costs calculation for the case study considered.

1050

1051

1052

1053

1054
1055 Figure 1. Schematic representation of the impact pathway approach (adapted from Van der Kamp
1056 and Bachmann, 2015).

1057
1058

- NO$_x$, PM$_{2.5}$, PM$_{10}$ emission flow (present and alternative scenario)
- Emission source geometry and location (present and alternative scenario)

DIDEM integrated model

CALPUFF dispersion model

- Delta-concentration maps of NO$_x$, PM$_{2.5}$, PM$_{10}$
- Delta-external costs distribution map
- Tables of overall delta-external costs, including uncertainty estimates

Figure 2. DIDEM model input and output.

- Emission source geometry and location
- Emission parameters (speed, temperature)
- Raw emission flow (NO_x, $PM_{2.5}$, PM_{10})

⟹ **Module 1 – extract.m** ⟹

- Corrected and formatted emission flow (NO_x, $PM_{2.5}$, PM_{10})

Module 2 – pte_bae_gen.m ⟹

- 1-hour and 24-hour concentration grids of NO_x, $PM_{2.5}$, PM_{10}

Module 3 – calpost.m ⟹

- 1-hour and 24-hour grids of average delta-concentration (NO_x, $PM_{2.5}$, PM_{10})
- Dailiy maximum 1-hour mean delta-concentration of NO_x
- Maximum and minimum delta-concentrations

Module 4 – extern.m ⟹

- Delta-external costs distribution map
- Tables of overall delta-external costs and related uncertainty ranges
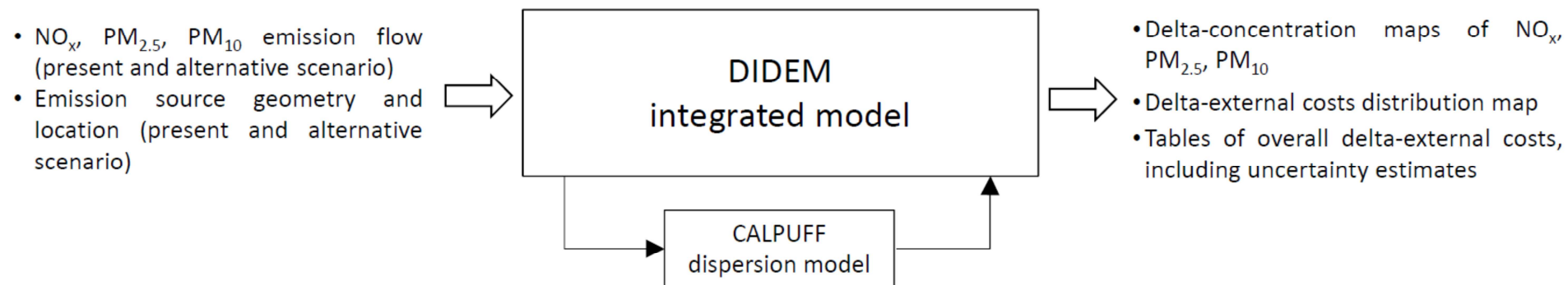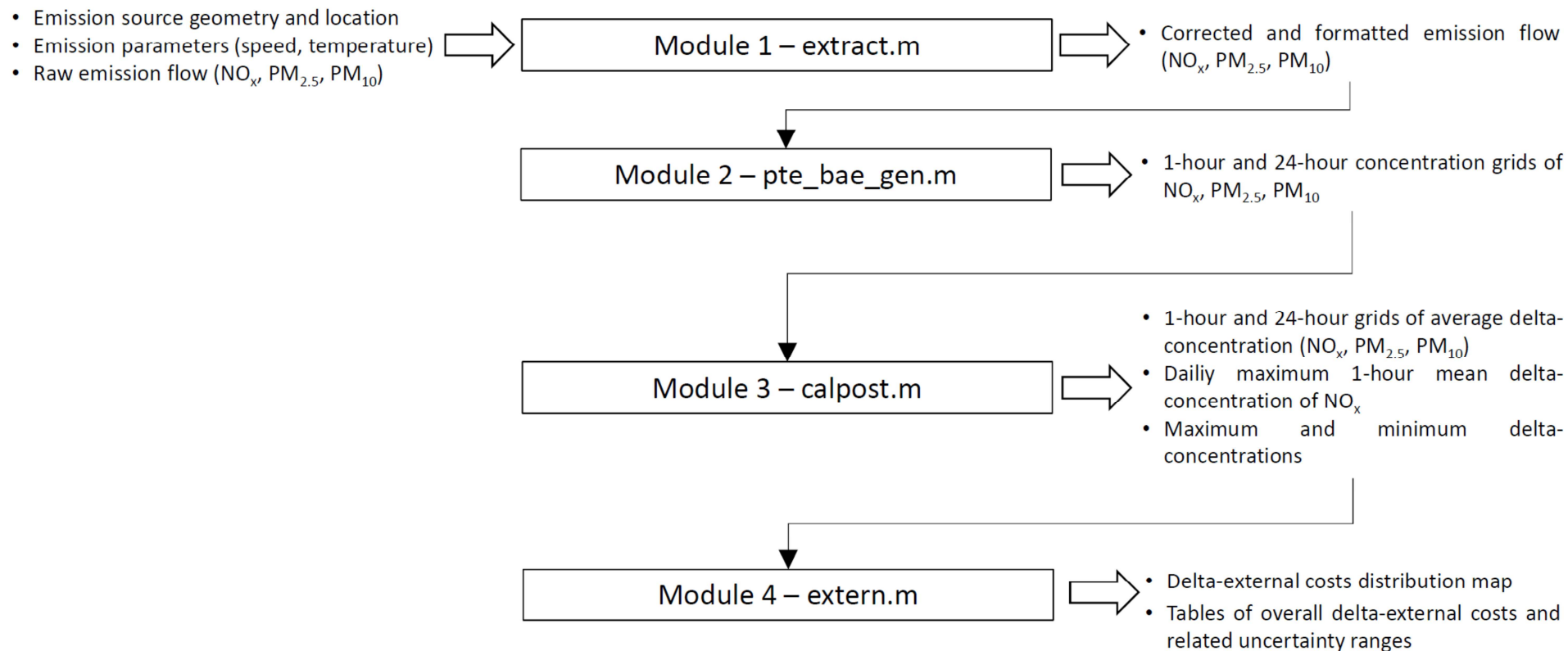
Figure 3. DIDEM model structure. Schematic representation of input and output from each Module.
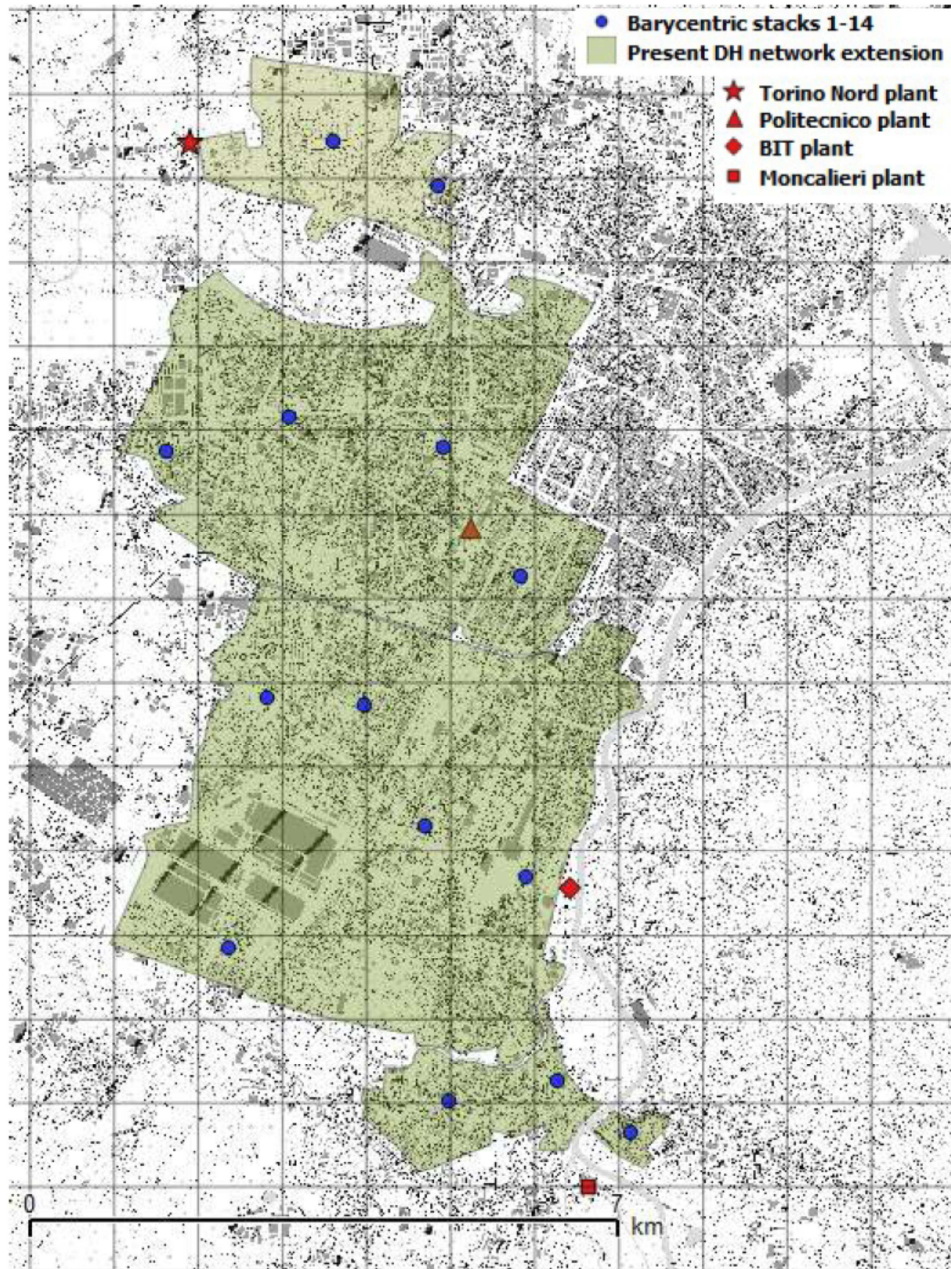
Figure 4. Present extension of Turin's DH network. Location of the plants powering the DH network. Location of the barycentric stacks assigned to the residential areas. The mesh grid represents the cells of the modelling domain.
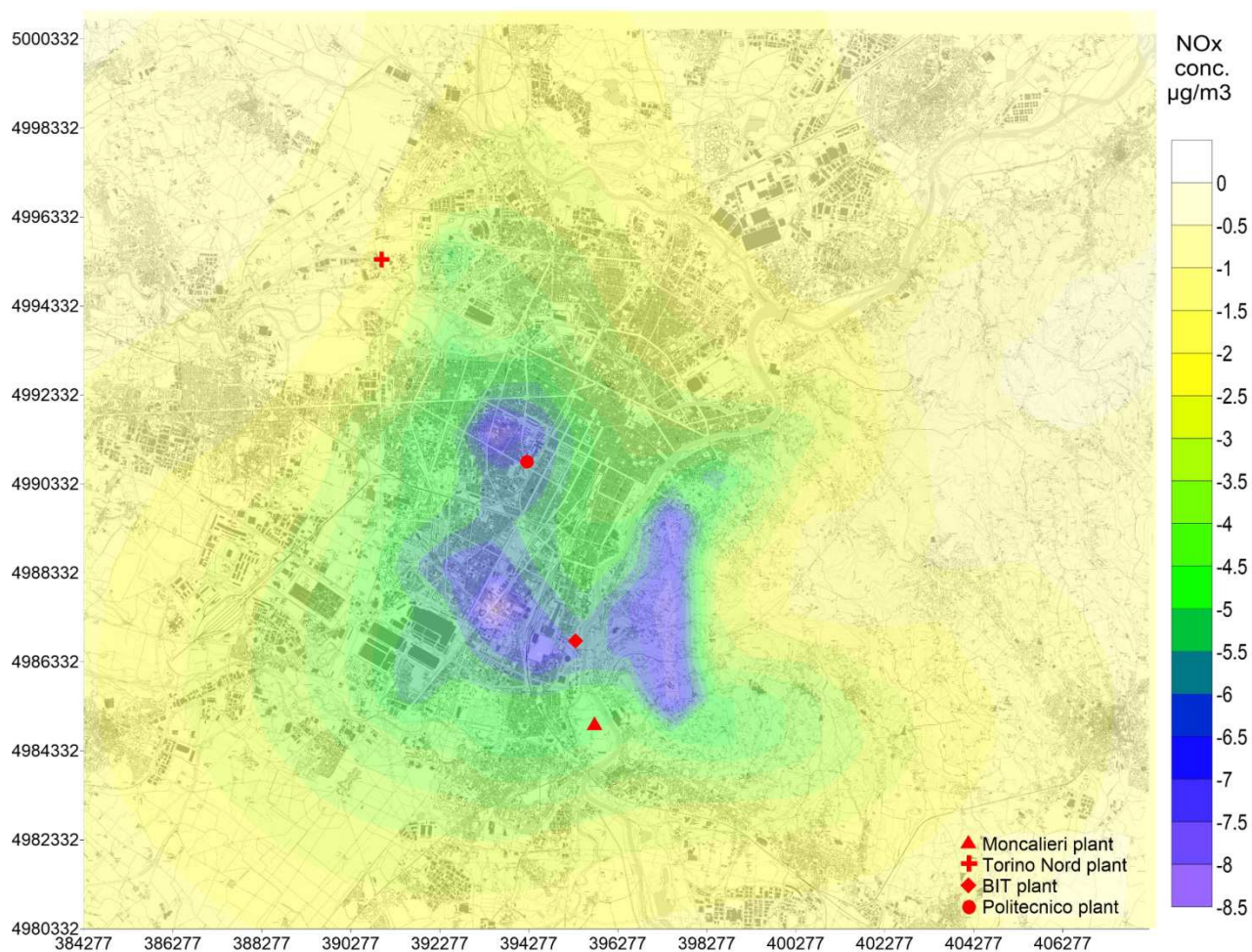
Figure 5. Average 1-hour delta-concentration map of NO_x in the metropolitan area of Turin, resulting from CALPUFF simulation. Average is calculated over the entire heating season (October to March).
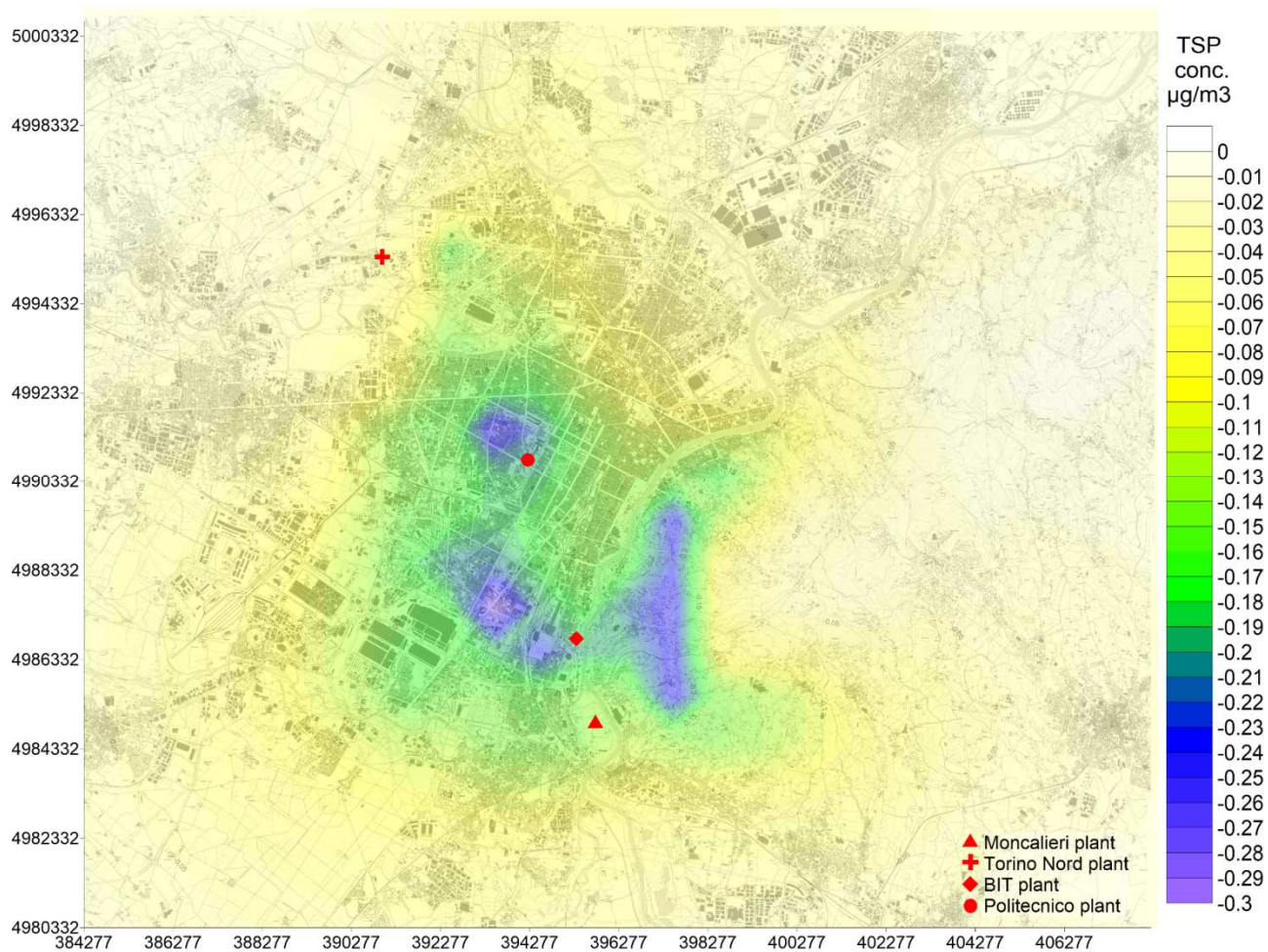
Figure 6. Average 1-hour delta-concentration map of total PM in the metropolitan area of Turin, resulting from CALPUFF simulation. Average is calculated over the entire heating season (October to March).
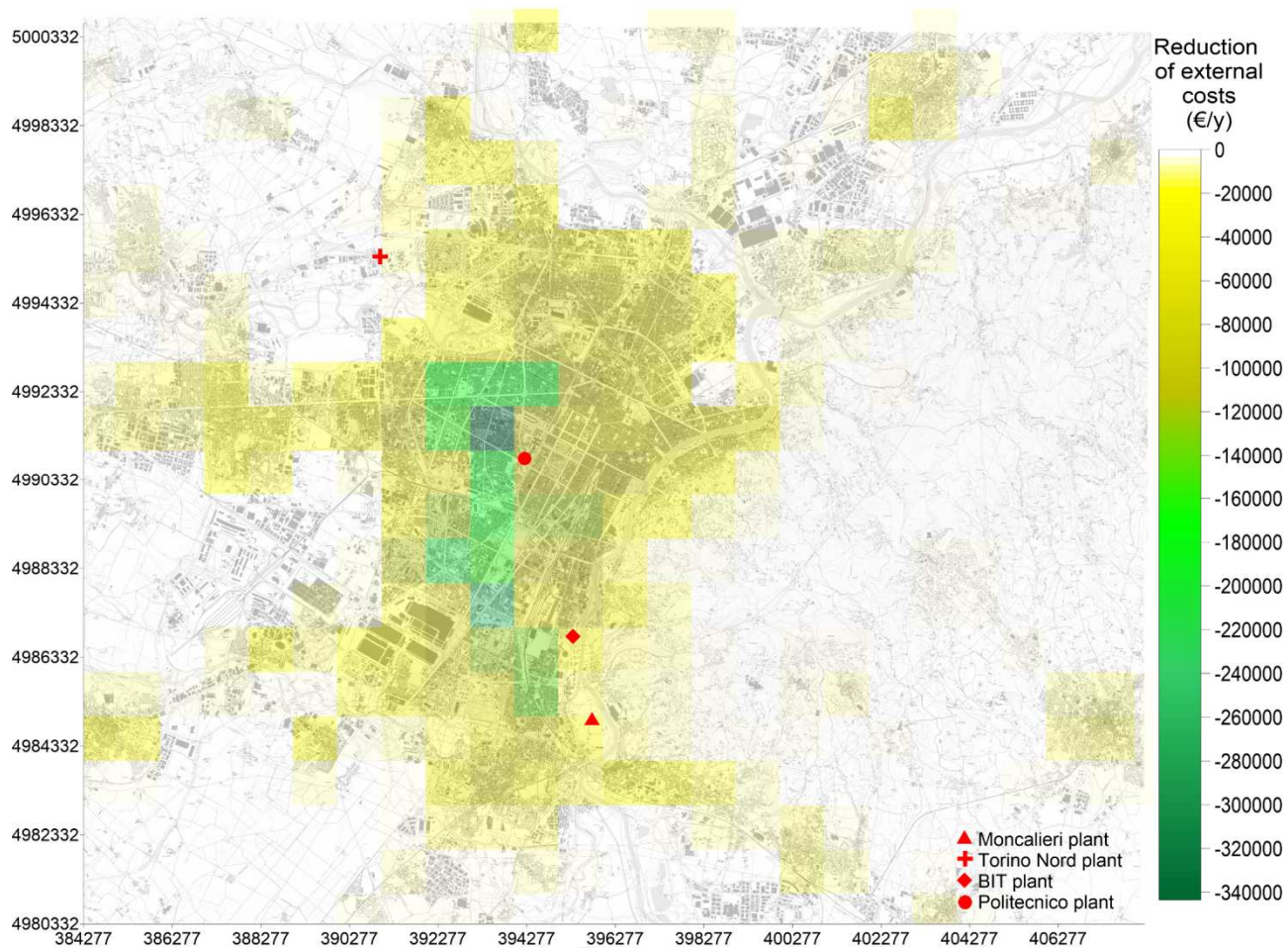
Figure 7. Map of average delta-external costs resulting from the integrated simulation with DIDEM model, referred to Setting 1.
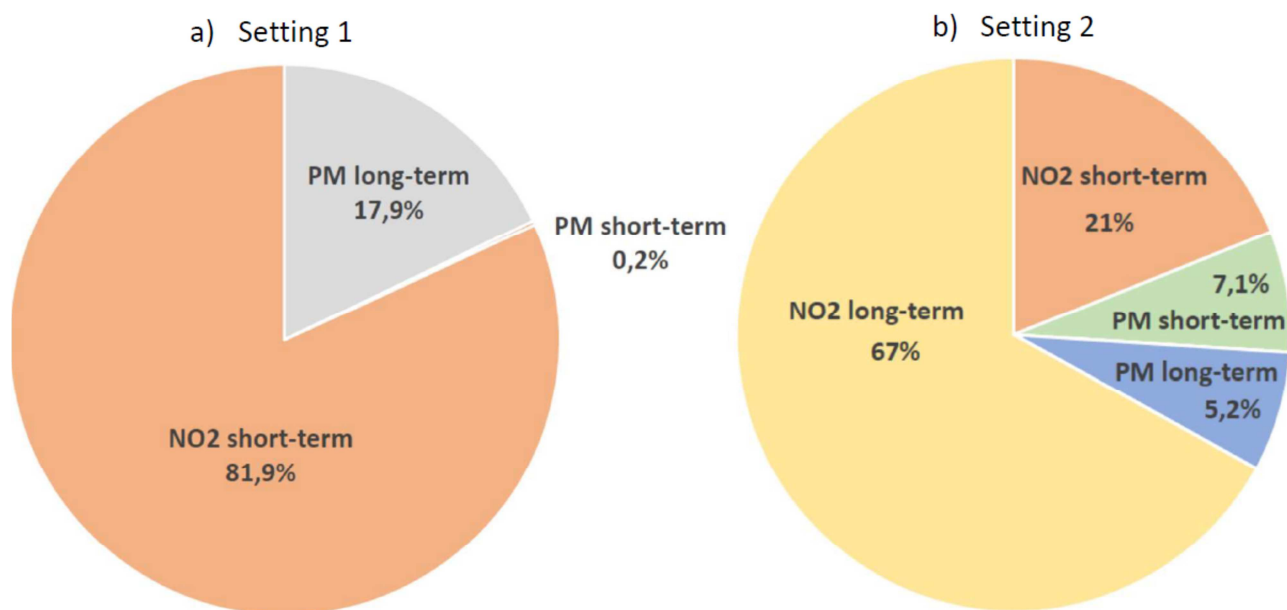
Figure 8. Case study results. Contribution of pollutant (NO_2 and PM) and exposure term (short and long term exposure) to the total delta-external costs, for Setting 1 (a) and Setting 2 (b) respectively.

Table 1. List of the pollutant-outcome pairs implemented in the DIDEM model, with the relative category of confidence level, average relative risk of the CRF and source of background health data (modified from WHO 2013a).

Pollutant metric	Health outcome	Group	Average RR per 10 µg/m³	Range of concentration	Source of background health data
PM, long-term exposure					
PM$_{2.5}$, annual mean	Mortality, all- cause (natural), age 30+ years	A*	1.062	All	European mortality database (MDB) (WHO HMDB), rates for deaths from all natural causes (International Classification of Diseases, tenth revision (ICD-10) chapters I–XVIII, codes A–R), latest available data
PM$_{2.5}$, annual mean	Mortality, cerebrovascular disease (includes stroke), ischaemic heart disease, chronic obstructive pulmonary disease (COPD) and trachea, bronchus and lung cancer, age 30+ years	A	1.07	All	European detailed mortality database (WHO HMDB), ICD-10 codes cerebrovascular: I60–I63, I65–I67, I69.0–I69.3; ischaemic heart disease: I20– I25; COPD: J40–J44, J47; trachea, bronchus and lung cancer: C33–C34, D02.1– D02.2, D38.1
PM$_{10}$, annual mean	Postneonatal (age 1–12 months) infant mortality, all-cause	B*	1.04	All	European Health for All database (WHO HFA-DB) and United Nations projections
PM$_{10}$, annual mean	Prevalence of bronchitis in children, age 6–12 years	B*	1.08	All	Mean prevalence from the Pollution and the Young (PATY) study: 18.6% (range 6–41%) (Gehring et al, 2006)
PM$_{10}$, annual mean	Incidence of chronic bronchitis in adults (age 18+ years)	B*	1.117	All	Annual incidence 3.9 per 1000 adults based on the Swiss Study on Air Pollution and Lung Disease in Adults (SAPALDIA; Schindler et al, 2009)
PM, short-term exposure					
PM$_{2.5}$, daily mean	Mortality, all-cause, all ages	A	1.0123	All	MDB (WHO HMDB)
PM$_{2.5}$, daily mean	Hospital admissions, cardiovascular diseases (CVDs) (includes stroke), all ages	A*	1.0091	All	European hospital morbidity database (WHO HMDB), ICD, ninth revision (ICD-9) codes 390-459; ICD-10 codes I00–I99

PM$_{2.5}$, daily mean	Hospital admissions, respiratory diseases, all ages	A*	1.0190	All	European hospital morbidity database (WHO HMDB), ICD-9 codes 460-519; ICD-10 codes J00–J99
PM$_{2.5}$, two-week average, converted to PM$_{2.5}$, annual average	Restricted activity days (RADs), all ages	B*	1.047	All	19 RADs per person per year: baseline rate from the Ostro and Rothschild (1989) study
PM$_{2.5}$, two-week average, converted to PM$_{2.5}$, annual average	Work days lost, working-age population (age 20–65 years)	B*	1.046	All	European Health for All database (WHO, HFA-DB)
PM$_{10}$, daily mean	Incidence of asthma symptoms in asthmatic children aged 5–19 years	B*	1.028	All	Prevalence of asthma in children based on "severe asthma" in the International Study on Asthma and Allergies in Childhood (ISAAC) (Lai et al., 2009)
NO$_2$, long-term exposure					
NO$_2$, annual mean	Mortality, all (natural) causes, age 30+ years	B*	1.055	>20 µg/m^3	MDB (WHO HMDB), rates for deaths from all natural causes (ICD-10 chapters I–XVIII, codes A–R) in each of the 53 WHO Regional Office for Europe countries, latest available data
NO$_2$, annual mean	Prevalence of bronchitic symptoms in asthmatic children aged 5–14 years	B*	1.021	All	Background rate of asthmatic children, "asthma ever", in Lai et al. (2009). Prevalence of bronchitic symptoms among asthmatic children 21.1% to 38.7% (McConnell et al., 2003)
NO$_2$, short-term exposure					
NO$_2$, daily maximum 1-hour mean	Mortality, all (natural) causes, all ages	A*	1.0027	All	MDB (WHO HMDB), rates for deaths from all natural causes (ICD-10 chapters I–XVIII, codes A–R) in each of the 53 countries of the WHO European Region, latest available data
NO$_2$, daily maximum 1-hour mean	Hospital admissions, respiratory diseases, all ages	A	1.0015	All	European hospital morbidity database (WHO HMDB), ICD-9 codes 460–519; ICD-10 codes J00–J99
NO$_2$, 24-hour mean	Hospital admissions, respiratory diseases, all ages	A*	1.0180	All	European hospital morbidity database (WHO HMDB), ICD-9 codes 460–519; ICD-10 codes J00–J99

Table 2. Monetary values implemented in the DIDEM model (from Holland, 2014b).

Health outcome	Monetary value (mean)	Monetary value (min)	Monetary value (max)	Unit
Mortality, age 30+ years	95,350	57,700	133,000	€$_{2005}$/YOLL
Infant mortality, age 1–12 months	2,450,000	1,600,000	3,330,000	€$_{2005}$/case
Bronchitis in children, age 6–18 years	588			€$_{2005}$/case
Chronic bronchitis in adults, age 18+ years	53,600			€$_{2005}$/case
Mortality, all ages	98,200	57,700	138,700	€$_{2005}$/YOLL
Hospital admissions, cardiovascular diseases, all ages	2,200			€$_{2005}$/admission
Hospital admissions, respiratory diseases, all ages	2,200			€$_{2005}$/admission
Restricted activity days (RADs), all ages	92			€$_{2005}$/day
Work days lost, working- age population (age 20–65 years)	130			€$_{2005}$/day
Asthma symptoms in asthmatic children, age 5–19 years	42			€$_{2005}$/case

Table 3. Data on power plants and emission sources presently feeding the DH network in Turin, Italy

Power plant	Emission source name and ID	Nominal power (th,el)	Stack height (m)	Stack diameter (m)	Latitude UTM ED50 (m)	Longitude UTM ED50 (m)
Moncalieri cogeneration combined cycle	1. Combined cycle RPW 2°GT (gas turbine)	395 MW_e 260 MW_t	60	7.5	395652.72	4983228.57
	2. Combined cycle RPW 3°GT (gas turbine)	383 MW_e 260 MW_t	60	7.0	395736.12	4983266.35
	3. Reserve boilers n°1-2-3	47 MW_t x 3	70	1.5	395624.74	4983162.38
Torino Nord cogeneration combined cycle	4. Combined cycle RPW 2°GT (gas turbine)	400 MW_e 220 MW_t	60	6	390950.42	4995655.77
	5. Integration and reserve boilers n°1-2-3	113 MW_t x 3	60	1.8	390975.80	4995571.70
BIT integration and reserve plant	6. Integration and reserve boilers n°1-2-3	85 MW_t x 3	43	1.8	395378.47	4985746.22
Politecnico integration and reserve plant	7. Integration and reserve boilers n°1-2-3	85 MW_t x 3	50	1.8	394275.49	4990844.94

Table 4. Energy and pollutants emission balance for the case study considered, present scenario year 2016.

Variable	Unit	Value
Fuel consumption for electricity and heat	GWh	9,992
Net electricity production	GWh	5,040
Net heat production for building heating	GWh	1,813
NO_x emission	t	327.7
Total PM emission	t	16.3

Table 5. Energy and pollutants emission balance for the case study considered, alternative scenario year 2016.

Variable	Unit	Value
Fuel consumption for heat production	GWh	3,705
Net heat production for building heating	GWh	1,813
NO_x emission	t	444.6
Total PM emission	t	16.1

Table 6. Result of delta-external costs calculation for the case study considered.

Confidence level on CRF data (Setting)	Delta external costs MEAN (€/y)		Delta external costs MINIMUM (€/y)		Delta external costs MAXIMUM (€/y)	
	€/y	€cent/kWh	€/y	€cent/kWh	€/y	€cent/kWh
High (Setting 1, Group A)	- 8,550,000	-0.472	- 3,880,000	-0.214	- 12,245,000	-0.675
Medium (Setting 2, Group A+B)	- 58,815,000	-3.244	- 32,245,000	-1.778	- 85,652,000	-4.724

Highlights

- Air pollution represents a continuous hazard to human health
- A new model is presented for comparing external costs of air pollution scenarios
- This tool integrates CALPUFF dispersion model with the latest WHO recommendations
- The model was tested on a real case study and compared to other existing tools
- Its application at the local scale may provide support to decision-makers